

1 **Single-colony sequencing reveals phylosymbiosis, co-phylogeny, and horizontal gene  
2 transfer between the cyanobacterium *Microcystis* and its microbiome**

3

4 Olga M. Pérez-Carrascal<sup>1</sup>, Nicolas Tomas<sup>1</sup>, Yves Terrat<sup>1</sup>, Elisa Moreno<sup>1</sup>, Alessandra Giani<sup>2</sup>, Laisa  
5 Corrêa Braga Marques<sup>2</sup>, Nathalie Fortin<sup>3</sup>, and B. Jesse Shapiro<sup>1,4,5</sup>

6

7 <sup>1</sup>Département de Sciences Biologiques, Université de Montréal, Montréal, Québec, Canada;

8 <sup>2</sup>Federal University of Minas Gerais, Belo Horizonte, Minas Gerais, Brazil; <sup>3</sup>National Research

9 Council of Canada, Montreal, Québec, Canada; <sup>4</sup>Department of Microbiology & Immunology,

10 McGill University, Montreal, Québec, Canada; <sup>5</sup>McGill Genome Centre, McGill University,

11 Montreal, Québec, Canada.

12

13 O.M.P.C. and N.T. contributed equally to this work.

14

15 \* Address correspondence to B. Jesse Shapiro, Olga M. Pérez-Carrascal or Nicolas Tomas,

16 <sup>1</sup>Département de Sciences Biologiques, Université de Montréal, Campus MIL, 1375 avenue

17 Thérèse-Lavoie-Roux, Montréal, QC, Canada H2V 0B3.

18 email: [jesse.shapiro@mcgill.ca](mailto:jesse.shapiro@mcgill.ca), [olga.maria.perez-carrascal@umontreal.ca](mailto:olga.maria.perez-carrascal@umontreal.ca) or

19 [nicolas.tomas@umontreal.ca](mailto:nicolas.tomas@umontreal.ca)

20

21

22

23

24 **Abstract**

25

26 Cyanobacteria from the genus *Microcystis* can form large mucilaginous colonies with attached  
27 heterotrophic bacteria – their microbiome. However, the nature of the relationship between  
28 *Microcystis* and its microbiome remains unclear. Is it a long-term, evolutionarily stable  
29 association? Which partners benefit? Here we report the genomic diversity of 109 individual  
30 *Microcystis* colonies – including cyanobacteria and associated bacterial genomes – isolated *in situ*  
31 and without culture from Lake Champlain, Canada and Pampulha Reservoir, Brazil. We found 14  
32 distinct *Microcystis* genotypes from Canada, of which only two have been previously reported,  
33 and four genotypes specific to Brazil. *Microcystis* genetic diversity was much greater between than  
34 within colonies, consistent with colony growth by clonal expansion rather than aggregation of  
35 *Microcystis* cells. We also identified 72 bacterial species in the microbiome. Each *Microcystis*  
36 genotype had a distinct microbiome composition, and more closely-related genotypes had more  
37 similar microbiomes. This pattern of phylosymbiosis could be explained by co-phylogeny in two  
38 out of the nine most prevalent associated bacterial genera, *Roseomonas* and *Rhodobacter*,  
39 suggesting long-term evolutionary associations. *Roseomonas* and *Rhodobacter* genomes encode  
40 functions which could complement the metabolic repertoire of *Microcystis*, such as cobalamin and  
41 carotenoid biosynthesis, and nitrogen fixation. In contrast, other colony-associated bacteria  
42 showed weaker signals of co-phylogeny, but stronger evidence of horizontal gene transfer with  
43 *Microcystis*. These observations suggest that acquired genes are more likely to be retained in both  
44 partners (*Microcystis* and members of its microbiome) when they are loosely associated, whereas  
45 one gene copy is sufficient when the association is physically tight and evolutionarily long-lasting.

46

47    Keywords: *Microcystis*, cyanobacteria, phylosymbiosis, co-phylogeny, microbiome.

48

49    Running head: Phylosymbiosis in the *Microcystis* microbiome

50

51 **Introduction**

52 Cyanobacteria occur naturally in aquatic ecosystems, often multiplying into harmful blooms and  
53 producing a diversity of toxins, which can cause severe human illness<sup>1</sup>. Many cyanobacteria and  
54 eukaryotic algae grow in mucilaginous colonies surrounded by a zone, called the phycosphere,  
55 rich in cell exudates, where metabolites are exchanged between numerous microorganisms<sup>2,3</sup>. In  
56 this microhabitat, the interactions between cyanobacteria and associated bacteria (AB) might  
57 include mutualism (with all partners benefitting), competition (with all partners competing for  
58 resources), antagonism (inhibiting one of the partners), commensalism (with one partner  
59 benefitting) and parasitism (with one partner benefitting at the expense of the other)<sup>3-5</sup>. However,  
60 the drivers shaping these associations are largely unknown. In some cases, AB may enhance algal  
61 or cyanobacterial growth<sup>6,7</sup>, aiding phosphorus acquisition in *Trichodesmium*<sup>8,9</sup>. Understanding the  
62 contributions of AB to cyanobacterial growth and toxin production has implications for our ability  
63 to predict and control harmful blooms.

64

65 *Microcystis* is a globally-distributed, often toxicogenic bloom-forming freshwater cyanobacterium,  
66 which forms macroscopic mucilaginous colonies. These colonies offer a nutrient-rich habitat for  
67 other bacteria, while also providing physical protection against grazers<sup>10-12</sup>. The *Microcystis*  
68 colony microbiome is distinct from the surrounding lake bacterial community, enriched in  
69 Proteobacteria and depleted in Actinobacteria<sup>13,14</sup>. The microbiome composition has been  
70 associated with temperature, seasonality, biogeography, *Microcystis* morphology and density<sup>13,15-</sup>  
71 <sup>17</sup>. Lab experiments show the potential for AB to influence *Microcystis* growth and colony  
72 formation<sup>18-21</sup>. Yet it remains unclear whether such interactions are relevant in natural settings, and  
73 if they are the product of long-term associations over evolutionary time.

74

75 Phylosymbiosis, a pattern in which microbiome composition mirrors the host phylogeny<sup>22</sup>,  
76 provides a useful concept for the study of host-microbiome interactions. Phylosymbiosis could  
77 arise from some combination of (1) vertical transmission of the microbiome from parent to  
78 offspring, resulting in co-speciation and shared phylogenetic patterns (co-phylogeny), (2)  
79 horizontal transmission of the microbiome, but with strong matching between hosts and  
80 microbiomes at each generation, and (3) co-evolution, in which hosts and microbiomes mutually  
81 impose selective pressures and adapt to each other. Distinguishing the relative importance of these  
82 three possibilities can be challenging, but in all cases the associations between hosts and  
83 microbiomes are non-random. Phylosymbiosis is typically studied between plant or animal hosts  
84 and their microbiomes<sup>23-25</sup> but *Microcystis* could also be considered a host, since it constructs the  
85 mucilage environment – although it is unclear to what extent it selects its AB or *vice versa*.  
86 *Microcystis* colonies are more open to the outside environment compared to mammalian guts, for  
87 example. Consequently, they might behave more like coral mucus<sup>25</sup> or other animal surfaces which  
88 seem to show weaker phylosymbiosis than guts<sup>26</sup>. The enclosed nature of animal guts reduces  
89 dispersal of microbiomes and favours vertical transmission, potentially leading to co-phylogeny  
90 without the need to invoke co-evolution<sup>27</sup>. In contrast, metagenomic sequencing suggests  
91 *Microcystis* and its microbiome are globally distributed<sup>16</sup>, making it unlikely that phylosymbiosis  
92 could arise due to common biogeography of *Microcystis* and its microbiome. On the other hand,  
93 *Microcystis* may be geographically structured on shorter evolutionary time scales, due to local  
94 adaptation or clonal expansions, and *Microcystis* genotypes might have distinct phenotypic  
95 characteristics that could select for distinct microbiomes<sup>28,29</sup>. Phylosymbiosis studies to date are

96 biased toward the gut relative to external host compartments<sup>22</sup>, and *Microcystis* colonies provide  
97 an ideal model of a more 'external microbiome'.

98  
99 Previous studies of the *Microcystis* microbiome have used either culture-independent  
100 metagenomics from lakes, a bulk biomass collection method which cannot resolve fine-scale  
101 spatial interaction within colonies (e.g.,<sup>16</sup>), or culture-based studies of *Microcystis* isolates, which  
102 have found host-microbiome divergence according to phosphorous gradients and taxonomy<sup>30</sup>, but  
103 may not be representative of the natural diversity of *Microcystis* or AB as they occur in nature. To  
104 combine the strengths of both these approaches, we developed a simple method for isolating  
105 individual *Microcystis* colonies directly from lakes, followed by DNA extraction and sequencing  
106 without a culture step<sup>29</sup>. Here we applied this method to 109 individual colonies from Lake  
107 Champlain, Canada and Pampulha Reservoir, Brazil, yielding 109 *Microcystis* genomes and 391  
108 AB genomes.

109  
110 Our findings reveal an expanded *Microcystis* genotypic diversity, and a *Microcystis* colony  
111 microbiome shaped by the host genotype, resulting in a significant signature of phylosymbiosis.  
112 We inferred co-speciation of *Microcystis* with two of the most prevalent genera in its microbiome  
113 (*Rhodobacter* and *Roseomonas*) suggesting evolutionarily stable associations. We also inferred  
114 extensive horizontal gene transfer (HGT) events among *Microcystis* and its microbiome, mainly  
115 involving lower-fidelity partners than *Rhodobacter* and *Roseomonas*. Overall, our results suggest  
116 ecologically and evolutionarily stable associations between *Microcystis* and members of its  
117 microbiome.

118

119 **Results**

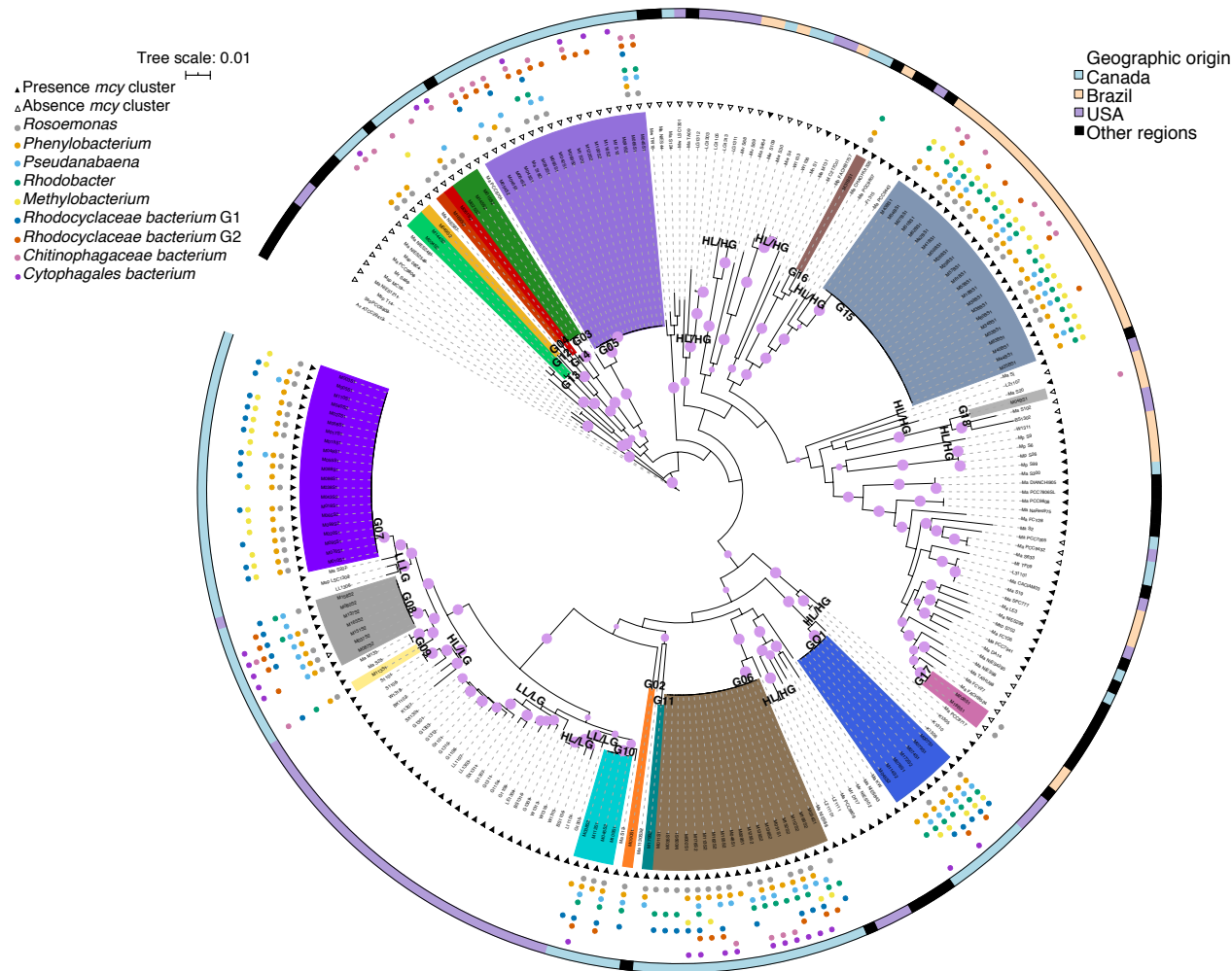
120

121 **Genotypic diversity of *Microcystis* colonies in Lake Champlain and Pampulha Reservoir.**

122 To study the relationship between *Microcystis* and its AB in natural settings, we sequenced 109  
123 individual *Microcystis* colonies from 16 lake samples (82 colonies from Lake Champlain, Quebec,  
124 Canada and 27 from Pampulha Reservoir, Minas Gerais, Brazil; Supplementary Table 1).  
125 *Microcystis* genomes were assembled and binned separately from AB genomes (Methods), which  
126 we will describe below. Consistent with our previous study of *Microcystis* isolate genomes<sup>29</sup>,  
127 nearly all *Microcystis* genomes share  $\geq 95\%$  average nucleotide identity (ANI), with the exception  
128 of 14/53,381 genome pairs with ANI  $< 94.5\%$ . The 95% ANI threshold is typically used to define  
129 bacterial species, but we previously found significant phylogenetic substructure above 95% ANI,  
130 coherent with multiple species or ecotypes within *Microcystis*<sup>29</sup>. Consistent with such fine genetic  
131 structure within our sampled colonies, we identified 18 monophyletic, closely-related genotypes  
132 of *Microcystis* ( $\geq 99\%$  ANI; Supplementary Table 2 and Fig. 1). These genotypes (highlighted  
133 clades in Fig. 1) are nested within the phylogeny of 122 isolate genomes previously sampled from  
134 North America, Brazil, and worldwide. However, only two genotypes (G05 and G10) have been  
135 observed in culture previously, possibly due to the fine-grained definition of genotypes ( $\geq 99\%$   
136 ANI) combined with undersampling of natural diversity in culture collections<sup>31</sup>. Consistent with  
137 previously observed biogeographic patterns between North and South America<sup>29</sup>, we found 14  
138 genotypes unique to Lake Champlain, and four unique to Pampulha, with no genotypes found in  
139 both locations.

140

141 *Microcystis* is thought to be adapted to high nutrient conditions, since it often blooms in eutrophic  
142 waters such as Champlain and Pampulha (Supplementary Table 3). However, a recent sampling  
143 of Michigan lakes identified *Microcystis* isolates adapted to low-phosphorus (low-phosphorus  
144 genotypes, LG), which occur in both high- and low-phosphorus lakes<sup>30</sup>. Genotypes G07, G08, G09  
145 and G10 from Lake Champlain are nested within the LG clade with high bootstrap support (Fig.  
146 1), indicating that low-phosphorus-adapted genotypes also occur in high-phosphorus lakes.  
147 Notably, most of the genomes within the LG clade (66 out of 67) encode the *mcy* gene cluster  
148 required for the biosynthesis of the cyanotoxin microcystin<sup>32</sup>. In contrast to the single LG clade,  
149 high-phosphorus genotypes (HG), are broadly distributed across the phylogenetic tree, recovered  
150 from multiple geographic locations, and some but not all encode *mcy* (Fig. 1). This pattern of *mcy*  
151 presence/absence is consistent with multiple *mcy* gene gain/loss events, mostly occurring in deep  
152 internal branches of the phylogeny, such that closely-related genotypes tend have identical *mcy*  
153 gene profiles.



154

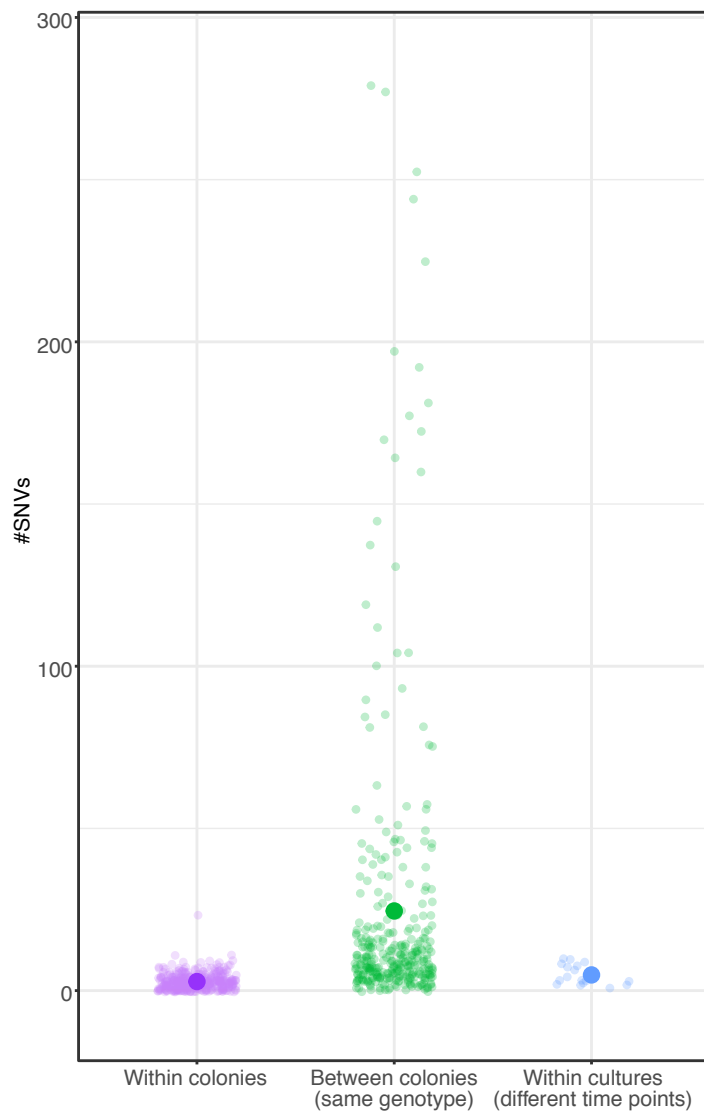
155 **Figure 1. Maximum likelihood phylogenetic tree of 109 *Microcystis* colony genomes and previously**  
156 **sequenced reference genomes.** *Microcystis* genomes were classified in 18 genotypes based on Average  
157 Nucleotide Identity (ANI) greater or equal to 99%. A core genome was inferred based on 109 *Microcystis*  
158 genomes and 122 *Microcystis* reference genomes downloaded from NCBI. The alignment of the 115 core  
159 genes (68,145 bp in total after excluding positions with gaps) was used to infer the Maximum Likelihood  
160 phylogeny. The tree was rooted using two cyanobacteria (*Anabaena variabilis* ATCC29413 and  
161 *Synechocystis* sp. PCC6803) as outgroups. The clades highlighted in different colours indicate *Microcystis*  
162 genotypes (G01 to G18) from this study; uncolored clades are other reference genomes from the literature.  
163 The purple circles on the tree branches indicate bootstrap values greater or equal to 70%. The empty and

164 filled triangles around the tree indicate absence and presence of the *mcy* cluster, respectively. The small  
165 colored and filled dots indicate the most prevalent associated bacteria genera related to each *Microcystis*  
166 genome. The outermost circle indicates the geographic origin of the *Microcystis* genomes. Several  
167 references genomes of *Microcystis* genotypes recovered from environments with high- and low phosphorus  
168 are indicated as LL/LG (Low Phosphorus Lake/Low Phosphorus genotype), HL/LG (High Phosphorus  
169 Lake/Low Phosphorus Genotype) and HL/HG (High Phosphorus Lake/High Phosphorus Genotype).

170

171 **Lower *Microcystis* diversity within than between colonies of the same genotype suggests**  
172 **clonal colony formation.**

173 A previous study of Michigan lakes supported clonal colony formation (by cell division) in isolates  
174 from high-phosphorus lakes, but suggested a preponderance of nonclonal colonies (by  
175 agglomeration of distantly related cell) in low-phosphorus lakes<sup>30</sup>. To distinguish between clonal  
176 and nonclonal colony formation, we compared genetic diversity within and between colonies.  
177 Within colonies, the number of single nucleotide variants (SNVs) was significantly lower (mean  
178 of 3 SNVs) than between colonies (mean of 25) of the same genotype (Two-tailed Wilcoxon Rank  
179 Sum Test,  $P < 0.05$ ; twelve outliers with more than 300 variants between colonies were excluded,  
180 making the test conservative) (Fig. 2 and Supplementary Table 4). These outliers were found in  
181 colonies within the genotypes G05, G06, G08 and G13. To put these results in context, *Microcystis*  
182 evolved an average of 5 SNVs after ~6 years of culture, slightly more variation than observed  
183 within a colony but still ~5X less than observed between colonies of the same genotype (Two-  
184 tailed Wilcoxon Rank Sum Test,  $P < 0.05$ ). Overall, these results are consistent with colony  
185 formation occurring mainly by clonal cell division in Lake Champlain and Pampulha – at least  
186 under the sampled environmental conditions.



187

188 **Figure 2. Greater genetic diversity between than within *Microcystis* colonies.** The number of single  
189 nucleotide variants (SNVs) within and between *Microcystis* colonies of the same genotype are shown,  
190 compared to SNVs that occurred over ~6 years of *Microcystis* culture in the laboratory (Methods). Large  
191 points show mean values.

192

193 **Evidence for phylosymbiosis between *Microcystis* and its microbiome.**

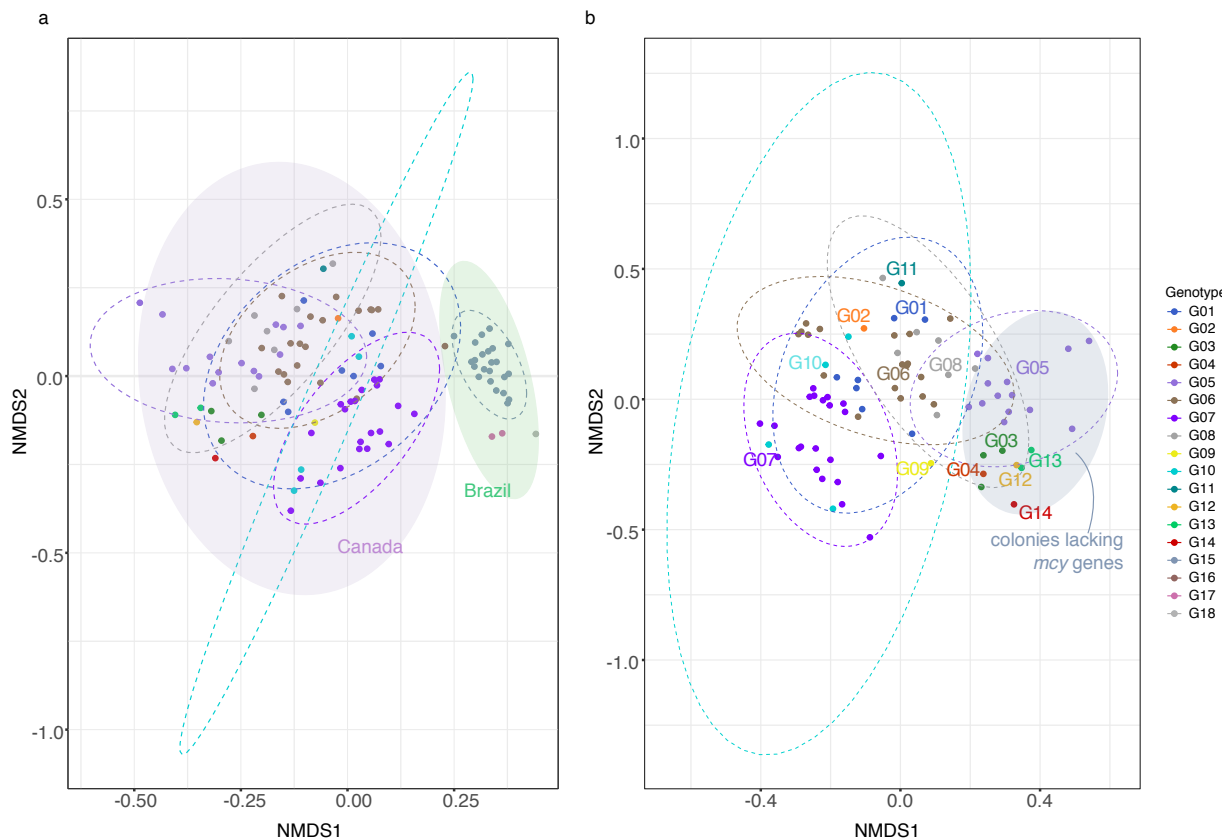
194 Having characterized the genetic diversity of *Microcystis* genomes, we turned our attention to the  
195 colony-associated bacteria (AB). We recovered a total of 391 high-quality non-*Microcystis*

196 genomes (Completeness  $\geq$  70 and contamination  $<$  10%) from the 109 colonies (Supplementary  
197 Table 1 and 5), classified into 72 putative species (ANI  $>$  95%) and 37 genera. Only five AB  
198 species were shared among colonies from Canada and Brazil: *Pseudanabaena* sp. A06,  
199 *Methylobacterium* sp. A30, *Roseomonas* sp. A21, *Burkholderia* sp. A55 (a likely contaminant, as  
200 discussed below) and *Gemmimonas* sp. A63 (Supplementary Fig. 2). Because certain low-  
201 abundance AB might be present in a colony but fail to assemble into a high-quality genome, we  
202 mapped reads from each colony to a database of all the AB genome assemblies and estimated AB  
203 genome coverages; each colony contained an average of six AB (genome coverage greater or equal  
204 to 1X), with a range of 0 to 15 (Supplementary Fig. 3). We found no strict "core" of AB present in  
205 all colonies, either at the species or genus level. However, several genera were quite prevalent.  
206 These include *Phenylobacterium* (present in 73.40% of colonies), *Roseomonas* (70.64%),  
207 *Pseudanabaena* (43.12%), *Rhodobacter* (46.79%), *Methylobacterium* (44.04%), *Rhodocyclaceae*  
208 G1 (unclassified genus) (39.45%), *Rhodocyclaceae* G2 (unclassified genus) (31.19%),  
209 *Chitinophagaceae* (unclassified genus) (26.60%) and *Cytophagales* (unclassified genus)  
210 (22.94%).

211  
212 To assess the evidence for phylosymbiosis, we first asked if different *Microcystis* genotypes had  
213 distinct colony microbiomes. The phylogeny illustrates how certain *Microcystis* genotypes  
214 appeared to be preferentially associated with particular AB (Fig. 1). For example,  
215 *Phenylobacterium* and *Methylobacterium* were present in all the colonies of genotype G15, while  
216 *Rhodobacter* and *Phenylobacterium* occur in all colonies of genotype G01. These anecdotal  
217 patterns are borne out in analyses of colony community structure, which show that *Microcystis*  
218 genotypes have distinct microbiomes (Fig. 3a). Genotype explains more variation in community

219 structure (PERMANOVA on Bray-Curtis distances,  $R^2 = 0.387$ ,  $P < 0.01$ ; Supplementary Table  
220 6) than any other measured variable including pH ( $R^2 < 0.05$ ) or temperature at the sampling site  
221 ( $R^2 < 0.05$ ), presence of microcystin (*mcy*) genes in the genotype ( $R^2 < 0.05$ ), or sampling site ( $R^2$   
222 = 0.11). Genotype was still the best explanatory variable when the analysis was performed on Lake  
223 Champlain samples only (Fig. 3b, PERMANOVA,  $R^2 = 0.309$ ,  $P = 0.001$ ). A key piece of evidence  
224 for phylosymbiosis is not only for microbiomes to differ among host lineages, but for microbiome  
225 composition to change proportionally to host phylogeny. To test this, we converted the *Microcystis*  
226 host phylogeny into a distance matrix, which we correlated with the colony microbiome Bray-  
227 Curtis dissimilarity matrix. Consistent with phylosymbiosis, we found that microbiome  
228 composition changes were correlated with the host phylogeny according to a Mantel test ( $r = 0.5$ ,  
229  $P = 0.001$ ) confirmed with Procrustean superimposition ( $r = 0.6$ ,  $P = 0.001$ )<sup>33</sup>.

230



231

232 **Figure 3. *Microcystis* genotypes have distinct microbiomes.** Non-metric multidimensional scaling  
233 (NMDS) plots are based on the coverage of the non-*Microcystis* metagenome-assembled genomes (MAGs)  
234 per colony (Bray–Curtis distance). **a)** All samples, including those from Pampulha, Brazil and Lake  
235 Champlain, Canada. Ellipses show 95% confidence intervals (stress = 0.202). **b)** Samples from Lake  
236 Champlain only (stress = 0.225). The grey shaded ellipse shows *Microcystis* colonies that do not encode  
237 the *mcy* cluster for microcystin toxin production.

238

239 ***Microcystis* genotype abundances vary over time in Lake Champlain and are correlated with  
240 prevalent members of the microbiome.**

241 *Microcystis* producers and non-producers of the cyanotoxin microcystin are known to change in  
242 relative abundance within lakes over time<sup>31,34,35</sup>. More generally, to what extent different

243 genotypes of *Microcystis* vary over time, along with their colony-associated bacteria, is less well  
244 known. We investigated the *Microcystis* genotype diversity in metagenomes from Lake Champlain  
245 based on 14 *Microcystis* genotypes identified in colonies from 2017 and 2018 (Fig. 1). Using a  
246 gene marker database of these 14 *Microcystis* genotypes (Methods), we estimated the relative  
247 abundance and read coverage of each genotype in 72 metagenomes from 2006 to 2018, sampled  
248 during the summer months (Supplementary Fig. 4). It is possible that these 14 genotypes do not  
249 represent the total genotypic diversity of *Microcystis* occurring in the lake. However, mapping  
250 metagenomic reads from the lake to these genotypes with a 99% sequence identity threshold  
251 allowed us to recover 93.5% of *Microcystis* reads (defining *Microcystis* at 96% sequence identity).

252

253 Using a distance-based redundancy analysis (dbRDA), we estimated the effect of total  
254 phosphorous, total nitrogen, dissolve phosphorous, dissolved nitrogen, mean temperature and time  
255 (years, months and season) on the *Microcystis* genotype community composition in the 42 Lake  
256 Champlain metagenomes with complete metadata, and with *Microcystis* genome coverage greater  
257 or equal to 1X. *Microcystis* genotype diversity in environmental metagenomes was best explained  
258 by yearly temporal variation ( $R^2 = 0.511$ ,  $P = 0.002$ ; Supplementary Fig. 5). Years did not differ  
259 significantly in their dispersion (PERMDISP  $P > 0.05$ ; Supplementary Table 6). Environmental  
260 variables such as nitrogen and phosphorus did not have a significant effect on the community  
261 composition. In a shorter time series (April to November of one year) in Pampulha, a more diverse  
262 community of four *Microcystis* genotypes eventually came to be dominated by one genotype (G15)  
263 encoding the *mcy* toxin biosynthesis gene cluster (Supplementary Fig. 6). However, more  
264 extensive sampling is required to estimate the effect of other environmental variables (i.e.,  
265 phosphorus) on the community composition in Brazil.

266

267 Similarly to *Microcystis* genotypes, the composition of AB in Lake Champlain also varied  
268 significantly across years (PERMANOVA, on Bray-Curtis distances,  $R^2 = 0.43$ ,  $P < 0.01$ ;  
269 Supplementary Fig. 7, stress = 0.1569). We asked if the presence of dominant *Microcystis*  
270 genotypes could explain the variation in the AB community composition. A significant effect of  
271 the genotype was observed using PERMANOVA ( $R^2 = 0.14$ ,  $P < 0.01$ ), but not using dbRDA ( $R^2$   
272 = 1.2,  $P > 0.05$ ). Years and *Microcystis* genotypes were the best explanatory variables for AB  
273 composition; however, their dispersions were significantly different ( $P < 0.01$ ) making the  
274 PERMANOVA results difficult to interpret. In addition, the AB community sampled from  
275 metagenomes includes both free-living and colony-attached AB, possibly adding noise to any  
276 signal of *Microcystis* genotypes selecting for specific AB within colonies.

277

278 We further hypothesized that the most prevalent AB in *Microcystis* microbiome should co-occur  
279 with *Microcystis* in lake metagenomes. In contrast, they should not co-occur with another  
280 cyanobacterium frequently observed in Lake Champlain, *Dolichospermum*, which serves as a  
281 negative control. We first estimated normalized read counts and coverage of *Microcystis*,  
282 *Dolichospermum* in the 72 metagenomes from the Lake Champlain time series (Supplementary  
283 Fig. 8). We then estimated the Spearman correlations between *Microcystis* or *Dolichospermum*  
284 and each AB species or genus. The two cyanobacteria were weakly correlated across the  
285 environmental metagenomes ( $r = 0.29$  and  $Q\text{-value} = 0.027$ , Spearman rank-based correlation test).  
286 As expected, the nine most prevalent AB genera in the *Microcystis* microbiome were strongly  
287 correlated with *Microcystis* ( $r > 0.7$ ,  $Q\text{-value} < 0.001$ ), and only weakly with *Dolichospermum* ( $r$   
288 < 0.4,  $Q\text{-value} > 0.001$ ) with the exception of *Phenylobacterium* ( $r = 0.47$ ,  $Q\text{-value} < 0.001$ ) which

289 is nevertheless more strongly associated with *Microcystis* (Supplementary Fig. 9). The positive  
290 correlation between the most prevalent AB genera and *Microcystis* was also supported using an  
291 alternative correlation method, SparCC, which corrects for compositional effects in the data ( $r >$   
292  $0.4$ ,  $Q\text{-value} < 0.05$ ) (Supplementary Table 7 and Fig. 9c). These significant positive correlations  
293 are consistent with close interaction between *Microcystis* and the most prevalent genera related to  
294 their microbiome. Genera found at lower prevalence in *Microcystis* colonies (e.g., *Phycisphaerales*  
295 *bacterium* (unclassified genus) and *Telmatospirillum*) were poorly correlated with both  
296 *Microcystis* and *Dolichospermum* (Supplementary Table 7 and Fig. 9a). Another AB belonging to  
297 the genus *Burkholderia* was quite prevalent in colonies but poorly correlated with *Microcystis* in  
298 metagenomes (present in the 40.37% of the colonies;  $r = -0.16$ ,  $Q\text{-value} = 0.343$ ) suggesting likely  
299 contamination of colonies rather than a true ecological association. However, such a signal of  
300 contamination was rare, suggesting that most of the data reflect true associations.

301

302 Finally, we asked if specific *Microcystis* genotypes were correlated with the presence of specific  
303 AB species (Supplementary Fig. 10) observed in *Microcystis* colonies. For example,  
304 *Rhodocyclaceae bacterium* G2 A13 was better correlated with genotype G05 than other  
305 *Microcystis* genotypes, consistent with the prevalence of this species in 13 out of 14 colonies of  
306 genotype G05. In contrast, genotype G10 was poorly correlated with certain species within the  
307 genera *Roseomonas* and *Methylobacterium* ( $r < 0.38$ ,  $Q\text{-value} > 0.001$ ). Overall, this is consistent  
308 with certain *Microcystis* genotypes having strong preferences for certain AB, while being  
309 unselective for others.

310

311 **Signatures of co-speciation between *Microcystis* and members of its microbiome.**

312 Phylosymbiosis can arise due to vertical inheritance of microbiomes, or horizontal acquisition of  
313 microbiomes at each generation, provided that host lineages are matched with distinct  
314 microbiomes. To assess the evidence for vertical inheritance of *Microcystis* AB, we used ParaFit  
315 to test for similarity between the *Microcystis* phylogeny and the phylogenies of the nine most  
316 prevalent AB genera strongly correlated with *Microcystis* but not with *Dolichospermum* in Lake  
317 Champlain (Supplementary Fig. 9). Each of these genera was represented by at least 12 high-  
318 quality draft genomes and was found in at least five different *Microcystis* genotypes. Significant  
319 co-phylogenetic signal suggests co-speciation of hosts and symbionts, consistent with a relatively  
320 long evolutionary history of association (e.g., vertical descent). We found that *Roseomonas*, the  
321 second most prevalent AB genus in colonies, and *Rhodobacter*, the third most prevalent, had  
322 significant signatures of co-phylogeny (Fig. 4), while *Phenylobacterium* and *Chitinophagaceae*  
323 were borderline cases (Table 1). Overall, there was no clear tendency for stronger co-phylogeny  
324 with more prevalent AB, or with AB most correlated with *Microcystis* over time in Lake  
325 Champlain metagenomes (Table 1). However, such tendencies would be hard to discern in this  
326 relatively small sample size. As expected, the likely contaminant *Burkholderia* A55 (*Burkholderia*  
327 *cepacia*) present in 40.37% of colonies, was poorly correlated with the presence of *Microcystis* in  
328 environmental metagenomes ( $r = -0.16$ ,  $Q\text{-value} = 0.343$ ), with no signal of co-phylogeny ( $P\text{-value}$   
329 = 0.732). Although co-phylogenetic signal was detectable in at least two of the most prevalent AB,  
330 the phylogenies are not identical (Fig. 4), suggesting a mixture of vertical and horizontal  
331 transmission. Even if horizontal transmission of AB among *Microcystis* lineages is likely, some  
332 degree of host-microbiome matching must be occurring to explain the co-phylogenetic signal.  
333  
334

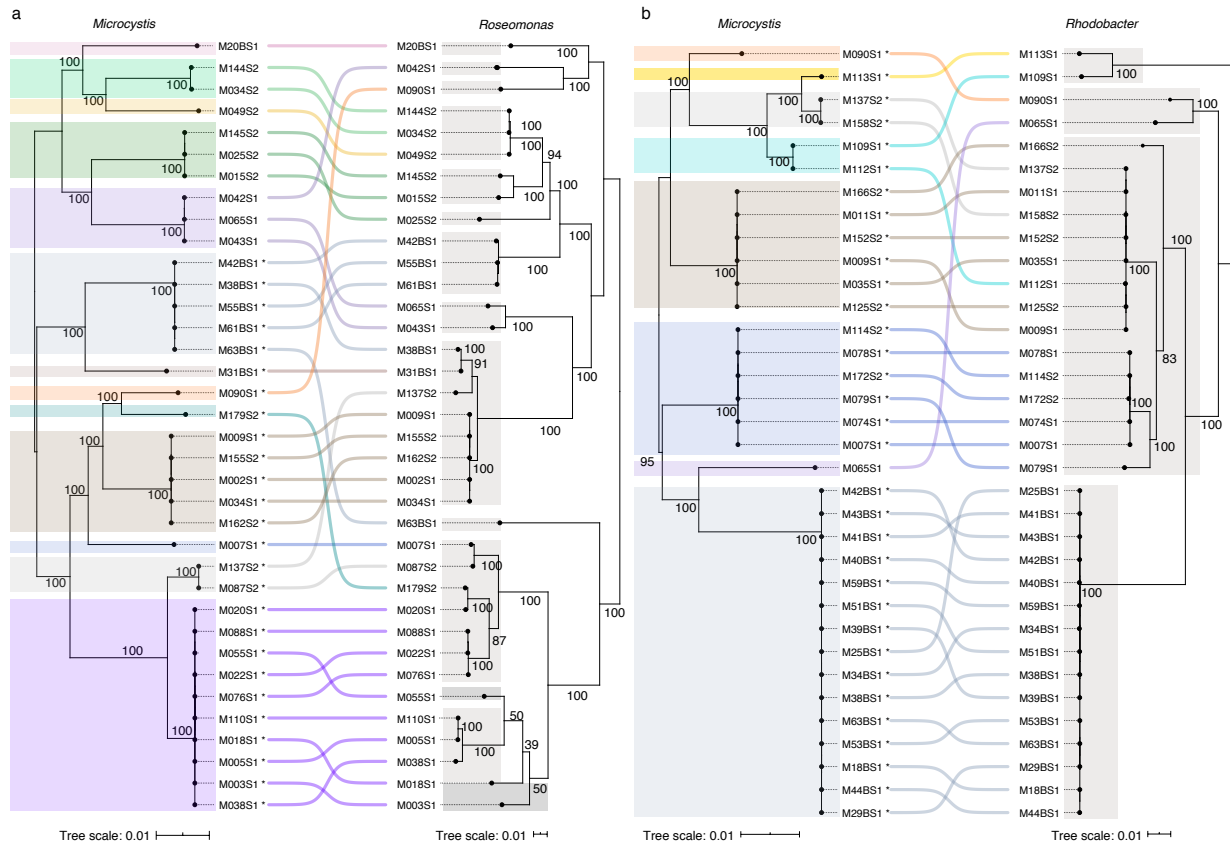
335 **Table 1.** Co-phylogeny analysis between *Microcystis* and the nine most prevalent associated bacterial  
336 genera within the *Microcystis* microbiome.

Associated bacteria (AB) genus	Number of species per genus	Number of AB genomes used in the phylogeny	Prevalence of AB in colonies from Canada and Brazil	Correlation with <i>Microcystis</i> in Canada metagenomes ( $r^2$ )	ParaFit test ( $P$ -values)
<i>Phenylbacterium</i>	5	60	73.40%	0.759 *	0.072 (0.008)
<i>Roseomonas</i>	13	36	70.64%	0.835 *	0.009** (0.001)
<i>Rhodobacter</i>	4	34	46.79%	0.779 *	0.0018** (0.0002)
<i>Methylobacterium</i>	3	29	44.04%	0.809 *	0.729 (0.081)
<i>Pseudanabaena</i>	2	20	43.12%	0.766 *	0.153 (0.017)
<i>Rhodocyclaceae bacterium G1</i>	2	19	39.45%	0.769 *	0.225 (0.025)
<i>Rhodocyclaceae bacterium G2</i>	2	21	31.19%	0.776 *	5.355 (0.595)
<i>Chitinophagaceae bacterium</i>	3	22	26.60%	0.795 *	0.081 (0.009)
<i>Cytophagales bacterium</i>	3	16	22.94%	0.740 *	0.702 (0.078)

337 \* significant correlation coefficients ( $Q < 0.01$ ).

338 \*\* significant  $P$ -values ( $P < 0.01$ ) (Bonferroni correction). Uncorrected  $P$ -values are shown between  
339 parentheses.

340



341

342 **Figure 4.** Co-phylogeny between *Microcystis* and two prevalent associated bacteria. (a) *Roseomonas* and  
 343 (b) *Rhodobacter* core genome phylogenies were compared to the *Microcystis* core phylogeny. The lines  
 344 between the two phylogenies connect genomes coming from the same *Microcystis* colony. The  
 345 phylogenetic trees for *Microcystis*, *Roseomonas* and *Rhodobacter* were based on 706, 135 and 470 core  
 346 genes, respectively. The different *Microcystis* genotypes are highlighted in colour, and the *Roseomonas* or  
 347 *Rhodobacter* species in gray. The asterisks indicate the presence of the *mcy* cluster. The co-phylogenetic  
 348 similarity is greater than expected by chance (ParaFit Global test,  $P\text{-value} < 0.01$ ).

349

### 350 **Horizontal gene transfer (HGT) between *Microcystis* and its associated bacteria**

351 Unrelated bacteria sharing a common environment, such as the human gut, are known to engage  
 352 in frequent horizontal gene transfer<sup>36</sup>. We hypothesized that *Microcystis* would also exchange  
 353 genes with members of its microbiome, which share a similar ecological niche – the colony milieu

354 – for at least some period of time. We began by using a simple heuristic to look for similar gene  
355 sequences ( $\geq 99\%$  amino acid identity) occurring in the *Microcystis* genome and at least one AB  
356 genome, as a proxy for relatively recent HGT events. Genome assembly and binning could affect  
357 this analysis by misplacing identical sequences either in *Microcystis* or in an AB genome, but not  
358 in both. To reduce this bias, we only considered a gene to be involved in HGT if it was present in  
359 at least four genomes. We identified a total of 1909 genes involved in HGT between *Microcystis*  
360 and one of seven AB species: *Pseudanabaena* A06, *Pseudanabaena* A07, *Burkholderiales*  
361 *bacterium* G3 A12, *Rhodocyclaceae bacterium* G2 A13, *Chitinophagaceae bacterium* A08,  
362 *Cytophagales bacterium* A04 and *Cytophagales bacterium* A05. Compared to the *Microcystis* core  
363 genome, these genes are enriched in functions related to secondary metabolite biosynthesis,  
364 replication and recombination, and defense mechanisms (Fig. 5). As a control, we repeated the  
365 analysis of HGT using the likely contaminant *Burkholderia* A55 genome instead of *Microcystis*.  
366 We identified 558 putative HGT events, of which 523 involving species not found to engage in  
367 HGT with *Microcystis*: *Methylobacterium* A30, *Rhodocyclaceae bacterium* G1 A54 and  
368 *Cupriavidus* A44. This suggests that *Microcystis* engages in more HGT with its microbiome than  
369 a random expectation (*i.e.* with a contaminant genome), and allows us to conservatively estimate  
370 the false-positive rate of HGT detection at 523/(523+1909), or 22%. Despite the significant noise,  
371 we expect the broad gene functional categories and specific AB involved in HGT with *Microcystis*  
372 to be relatively robust (Fig. 5). Surprisingly, prevalent AB with evidence of co-phylogeny with  
373 *Microcystis* (*Roseomonas* and *Rhodobacter*) shared relatively few (less than seven) HGT events  
374 with *Microcystis*. This counter-intuitive result could be explained if these co-phylogenetic  
375 associations are relatively ancient, but our HGT detection is biased toward recent events.  
376 Alternatively, it is possible that HGT is more likely among less intimately associated bacteria,

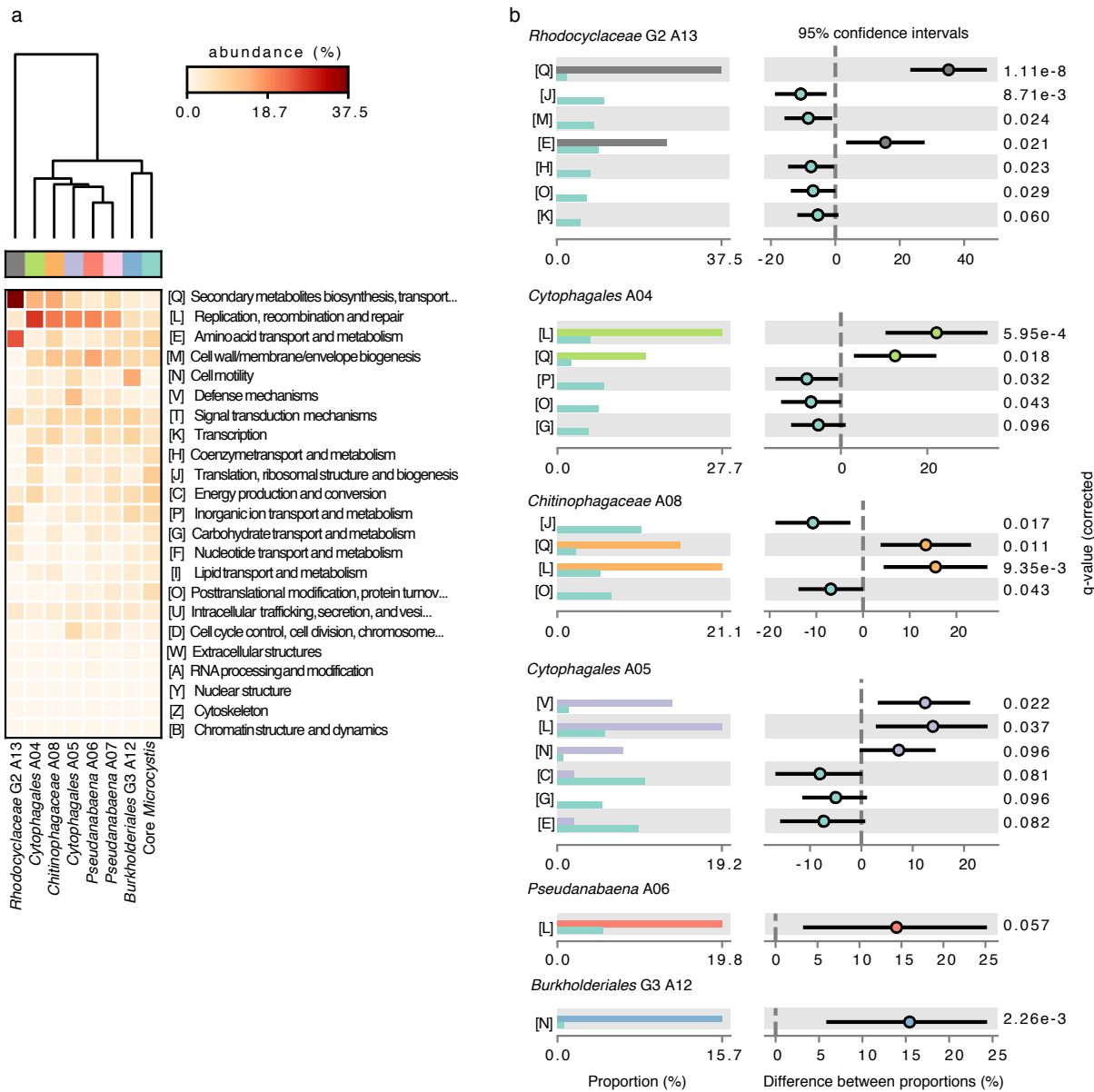
377 whereas an intimate association would select for only one, but not both partners, to encode the  
378 gene. This would also require that metabolites are shared between partners. Further work will be  
379 needed to thoroughly test this hypothesis.

380

381 As an additional validation of our HGT heuristic, we used Metachip, which uses phylogenetic  
382 incongruence in addition to a sequence identity threshold<sup>37</sup>. Metachip identified the same seven  
383 AB genera involved in HGT with *Microcysis* based on our simple heuristic, except for  
384 *Rhodocyclaceae bacterium* G2. However, Metachip is much more conservative, identifying only  
385 46 gene families involved in HGT (Supplementary Table 8). Of these gene families 31 were also  
386 identified by our heuristic method, suggesting they are high-quality candidates.

387

388



389

390 **Figure 5. Inferred recent HGT between *Microcystis* and associated bacteria.** Horizontal transferred  
 391 genes between *Microcystis* and each AB species were inferred with a simple heuristic and annotated in 23  
 392 Clusters of Orthologous Groups (COGs) functional categories using EggNOG mapper (Methods). **a)**  
 393 Clustering analysis based on the relative abundance of the genes for each functional category, compared to  
 394 the genes in the *Microcystis* core genome. **b)** COG functions showing differential abundance between  
 395 *Microcystis* core genes (turquoise) and the set of putative HGTs (other colors).

396

397 **Cellular functions encoded by members of the *Microcystis* microbiome.**

398 In contrast to genes shared by HGT, there may be a genetic division of labour between *Microcystis*  
399 and its microbiome, which would then be expected to encode different and complementary sets of  
400 gene functions. To compare these gene functions, we first characterized orthologous genes using  
401 the Kyoto Encyclopedia of Genes and Genomes (KEGG) orthologues (KO) in both *Microcystis*  
402 and its microbiome. Then, using the software ANTISMASH, we identified gene clusters involved  
403 in the biosynthesis of cyanopeptides and other pathways of interest. As expected for distantly  
404 related bacteria, *Microcystis* genotypes and AB encode distinct sets of gene functions  
405 (Supplementary Fig. 11). Bacteria from the same Phylum tend to cluster together in terms of their  
406 functional gene content. For example, *Microcystis* genotypes cluster with its fellow cyanobacteria  
407 *Pseudanabaena*, while Bacteroidetes (*i.e.* *Cytophagales* *bacterium* and *Chitinophagaceae*  
408 *bacterium*) formed a distinct cluster (Supplementary Fig. 11).

409

410 We identified several examples of possible functional complementarity between *Microcystis* and  
411 members of its microbiome. For example, *Microcystis* encodes incomplete pathways for the  
412 synthesis of biotin (M00123; pimeloyl-ACP/CoA => biotin) and cobalamin (M00122; cobinamide  
413 => cobalamin), suggesting that these functions might be subject to gene loss if the functions are  
414 provided by the microbiome. Consistent with this idea, AB encode complete pathways for both  
415 biotin (in *Cytophagales*, *Chitinophagaceae* and *Rhodocyclaceae*) and cobalamin (in *Rhodobacter*,  
416 *Azospirillum*, and *Bradyrhizobium*). Other AB (*e.g.*, *Roseomonas*, *Rhodobacter* and  
417 *Methylobacterium*) encoded genes involved in the anoxygenic photosynthesis (Supplementary  
418 Table 9) and genes related with the transport of rhamnose, D-xylose, fructose, glycerol and a-

419 glucoside, which could also complement the metabolic repertoire of *Microcystis*<sup>16</sup>, although this  
420 deserves further study.

421

422 *Roseomonas* and *Rhodobacter*, which show co-phylogeny with *Microcystis* but appear not to  
423 engage in significant amounts of HGT, are prime candidates for functional complementarity to  
424 have evolved and be maintained with high partner fidelity. Both these genera encode genes for the  
425 biosynthesis of carotenoids (phytoene desaturase (*crtI*) and phytoene synthase (*crtB*)). Carotenoid  
426 pigments like zeaxanthin are generally produced by *Microcystis* for their photoprotective  
427 properties and their capacity to improve the efficiency of photosynthesis.<sup>38</sup> Indeed, in our  
428 *Microcystis* genomes, we found genes encoding for phytoene synthase (*crtB*) and zeaxanthin  
429 glucosyltransferase (*crtX*). However, genes like (*crtI*), lycopene cyclase (*crtY*) and beta-carotene  
430 hydroxylase (*crtZ*) were only found in other AB genomes (e.g., *Cytophagales*). It is tempting to  
431 speculate that the *Microcystis* microbiome may also be involved in the production of these  
432 carotenoids. *Roseomonas* and *Rhodobacter* also have metabolic pathways for nitrogen fixation.  
433 *Microcystis* is unable to fix nitrogen, and previous studies have suggested it may rely on its  
434 microbiome for nitrogen<sup>16,39</sup>. The co-phylogenetic signal between *Microcystis* and these genera  
435 might thus be explained by these complementary functions.

436

437 **Discussion**

438

439 By combining single colony sequencing and metagenome analysis, we explored the genetic  
440 diversity of both *Microcystis* and its microbiome, and their variation over time in Lake Champlain,  
441 Canada and the Pampulha reservoir in Brazil. We revealed a higher diversity of *Microcystis*

442 genotypes than previously described<sup>40</sup>, and patterns of cophylogeny, phylosymbiosis and HGT  
443 between the host and its microbiome. Despite the absence of a core microbiome, several of the  
444 associations between *Microcystis* and its attached bacteria, notably *Roseomonas* and *Rhodobacter*,  
445 appear to be relatively stable over evolutionary time. These two genera have been previously  
446 reported to be correlated with *Microcystis* in environmental samples<sup>41,42</sup>. Whether these  
447 associations are beneficial to one or both partners remain to be seen, and deserve further study as  
448 possible targets for better predicting and controlling harmful *Microcystis* bloom events. For  
449 example, small filamentous cyanobacteria *Pseudanabaena* and members of the order  
450 *Cytophagales* have been previously reported as bloom biomarkers<sup>43</sup>.

451

452 There has been some debate about whether *Microcystis* colonies form by clonal cell division, or  
453 by aggregation of (potentially distantly related) cyanobacterial cells<sup>21,44</sup>. Consistent with another  
454 recent study in eutrophic lakes<sup>30</sup>, we conclude that clonal cell division is more likely, based on our  
455 observation of much greater genetic variation in the *Microcystis* genome between than within  
456 colonies of the same genotype. One caveat to this conclusion is that our limited and possibly biased  
457 sample of *Microcystis* colonies means that aggregated colonies could exist, but were unsampled  
458 due to small colony size (resulting in failure of DNA extraction). However, 93.5% of *Microcystis*  
459 metagenomic reads from Lake Champlain were recruited to our collection of colony genomes at  
460 99% nucleotide sequence identity, suggesting that the majority of natural *Microcystis* diversity is  
461 represented in our sample of colonies. Of course, these results are specific to Lake Champlain and  
462 should be replicated in other lakes under different environmental conditions (e.g., oligotrophic  
463 lakes).

464

465 Phylosymbiosis and co-speciation appear to be relatively common and strong in mammalian gut  
466 microbiomes<sup>22,23</sup>, and even in the more environmentally-exposed coral microbiome<sup>22,23</sup>. It is  
467 unclear if such tight and evolutionarily stable associations would apply to *Microcystis* and its  
468 associated bacteria, or if more transient interactions would prevail. While the idea of a *Microcystis*  
469 microbiome has been suggested previously based on bulk metagenomic and amplicon sequencing  
470 from lakes<sup>16,45</sup>, here we refine the *Microcystis* microbiome concept beyond co-occurrence patterns  
471 to physical association within a colony. We found that the most prevalent associated bacteria from  
472 individual *Microcystis* colonies also tend to co-occur with *Microcystis* over time in Lake  
473 Champlain. The composition of the microbiome varies along the *Microcystis* phylogenetic tree,  
474 consistent with phylosymbiosis and relatively long-term associations. At least two associated  
475 bacteria show significant co-phylogenetic signal, suggesting co-speciation with *Microcystis*.  
476 Therefore, although possibly not as strong as in mammals or even coral, phylosymbiosis and co-  
477 phylogeny are features of the *Microcystis* microbiome. Phylosymbiosis can arise as a consequence  
478 of shared biogeography between hosts and microbiomes<sup>46</sup>, and we do observe distinct  
479 microbiomes in Brazil and Canada. However, we found evidence for phylosymbiosis within a  
480 single lake in Canada, suggesting that other factors – such as host-microbiome trait matching – are  
481 likely at play.

482

483 As expected for distantly related bacteria, *Microcystis* and its associated bacteria encode different  
484 functional gene repertoires, some of which could be complementary and mutually beneficial. For  
485 example, we found that associated bacteria may complement biosynthetic functions that were lost  
486 or never present in *Microcystis*, such as biotin, cobalamin, or carotenoid synthesis. Carotenoids  
487 act as antioxidants and may increase the photosynthetic light absorption spectrum<sup>47,48</sup>. Some

488 associated bacteria, including the co-speciating *Roseomonas* and *Rhodobacter*, have metabolic  
489 pathways for nitrogen fixation and phosphonate transport. *Microcystis* is unable to fix nitrogen,  
490 and studies suggest that it may rely on nitrogen-fixing members of its microbiota<sup>16,39</sup>. While it  
491 remains unclear if metabolites are actually exchanged between *Microcystis* and members of its  
492 microbiome, these hypotheses could be tested experimentally.

493

494 Horizontal gene transfer (HGT) is relatively common in bacteria, and may occur among unrelated  
495 bacteria<sup>49</sup> particularly when they share an ecological niche such as the human gut<sup>36</sup>. *Microcystis* is  
496 physically associated with its microbiome for at least part of the colony life cycle, and we  
497 hypothesized that HGT could occur within colonies. Using two methods to detect HGT, we found  
498 evidence for gene transfers between *Microcystis* and at least six different species of associated  
499 bacteria: two species of *Pseudanabaena*, two *Cytophagales*, one *Burkholderiales*, and one  
500 *Chitinophagaceae* species. Notably, we did not find evidence for HGT between *Microcystis* and  
501 its two most co-phylogenetically associated bacteria, *Roseomonas* and *Rhodobacter*. To explain  
502 this result, we hypothesize that such long-term associations might favour the loss of redundant  
503 genes, as predicted by the Black Queen Hypothesis<sup>50</sup>. In other words, a gene needs to be encoded  
504 by only one partner, provided that gene products or metabolites are shared between partners.  
505 Therefore, even if HGT does occur between partners, we would not expect to find the same gene  
506 redundantly encoded in both partners. These evolved co-dependencies would further reinforce  
507 partner fidelity and could help explain the co-phylogenetic signal between them.

508

509 Overall, our results provide evidence for long-lasting eco-evolutionary associations between  
510 *Microcystis* and its microbiome. Some members of the microbiome may be more tightly associated

511 than others, and based on their gene content we hypothesize that they may provide beneficial and  
512 complementary functions to *Microcystis*. These hypotheses could be tested in experimental co-  
513 cultures, which have recently shown how the *Microcystis* microbiome can alter its competitive  
514 fitness against eukaryotic algae<sup>51</sup>. These experiments could be extended to the combinations of  
515 *Microcystis* genotypes and associated bacteria which we have shown to be intimately associated  
516 in nature.

517

## 518 **Methods**

519

### 520 **Sample collection and DNA extraction for colonies and metagenomes**

521 To access to the genomic diversity of *Microcystis* in Lake Champlain and Pampulha reservoir, 346  
522 individual *Microcystis* colonies were isolated across the bloom season (July to October in Quebec,  
523 Canada (45°02'44.86"N, 73°07'57.60"W) and April to November in Minas Gerais, Brazil  
524 (19°55'09"S and 43°56'47"W)). Colonies were isolated from surface water samples (~50 cm  
525 depth) after concentration using a plankton net (mesh size 20 µm). One liter of concentrated water  
526 was collected and stored at 4 °C for a maximum of 36 hours until colony isolation. Colonies were  
527 isolated using micropipes, sterile medium (Z8 medium) and a microscope (Nikon E200 Eclipse).  
528 Each colony was washed 15-20 times using sterile Z8 medium and stored at -80 C until DNA  
529 extraction. The DNA extraction was performed directly on each colony using the ChargeSwitch®  
530 gDNA Mini Bacteria Kit. Two additional steps were added to ensure the rupture of the *Microcystis*  
531 colonies and cells (See Supplementary Methods). Briefly, each colony was added to a tube  
532 containing 50 mg of beads (PowerBead tubes, glass 0.1 mm- Mo-bio), incubated with lysis  
533 solutions, and then vortexed using the TissueLyser LT (Qiagen) for three minutes at 45 oscillation

534 per second. The tube was then centrifuged for 1 minute at 9000 rcf. This procedure yielded DNA  
535 for 109 colonies, sequenced as described below. Matched water samples were collected at the same  
536 place and time as colonies, spanning 16 time points (Supplementary Table 10). Water temperature  
537 and pH were also measured at each sampling point.

538

539 For metagenomic sequencing, a total of 72 lake water samples were collected over 10 years (2006  
540 to 2018) during the ice-free season (April to November) from the photic zone of Missisquoi Bay  
541 at two different sites (littoral and pelagic) of Lake Champlain, Quebec, Canada (45°02'45"N,  
542 73°07'58"W). Lake water was filtered and DNA was extracted using a Zymo Kit (Zymo, D4023)  
543 as described previously<sup>43</sup>. The filtration was performed the same day of the sampling, using  
544 between 50 and 250 mL of water samples, depending on the amount of biomass, onto 0.2 µm  
545 hydrophilic polyethersulfone membranes (Millipore, Etobicoke, ON). Samples were obtained at  
546 relatively low frequency between 2006 and 2016, and at higher frequency (approximately weekly  
547 or more often) during bloom periods between 2015 and 2016 (Supplementary Table 3). Water  
548 samples corresponding to six sampling points from Minas Gerais Brazil were also collected for  
549 DNA extraction and metagenome sequencing. Environmental variables were measured for each  
550 sample. Sample water were collected (50 ml) for measuring nutrients (DN, DP, TP and TN), except  
551 for the samples from Brazil (Supplementary Table 3)<sup>43</sup>.

552

### 553 **DNA sequencing of single colonies and metagenomes**

554 DNA extracted from *Microcystis* single colonies was sequenced using the Illumina HiSeq 4000  
555 platform with 150bp paired-end reads. The sequencing libraries (with average fragment size  
556 360bp) were prepared using the NEB (New England Biolabs®) low input protocol. The DNA

557 extracted from filtered bulk lake water for each sampling point (2017 and 2018) from Canada and  
558 Brazil were sequenced using Illumina NovaSeq 6000 S4 platform with 150bp paired-end reads.  
559 The earlier lake water samples from a previous long-term experiment in Lake Champlain (2006 to  
560 2016) were sequenced using Illumina Hiseq2500 with 125 paired-end reads (Supplementary Table  
561 3).

562

### 563 **Metagenome assembly and genome binning**

564 For the *Microcystis* colonies, the sequencing reads were filtered and trimmed using Trimmomatic  
565 (v0.36)<sup>52</sup> then assembled with MEGA-HIT (v1.1.1)<sup>53</sup>, producing contigs belonging to both  
566 *Microcystis* and associated bacteria. We then used Anvi'o (v3.5) to filter, cluster and bin the  
567 contigs longer than 2,500 bp as was previously<sup>29,54</sup>. The quality of each resulting metagenome-  
568 assembled genome (MAG) was estimated using CheckM (v1.0.13)<sup>55</sup>. From the 109 colonies, 500  
569 medium and high-quality MAGS were identified (completeness  $\geq$  70% and contamination  $\leq$  10%)  
570 (Supplementary Table 1 and 5)<sup>56</sup>. MAGs were annotated using Prokka (v1.14.0)<sup>57</sup>. Pairwise  
571 average nucleotide identity (ANI) values between genomes were estimated using FastANI (v1.2)  
572 and pyani<sup>58,59</sup>. MAGs were classified into different taxonomic groups at a threshold of ANI  $\geq$  96%  
573 (Supplementary Table 5 and 11). MAGs were assigned to genera and species using Blastp of the  
574 recA and RpoB proteins against the NCBI database, and refined using the Genome Taxonomy  
575 Database Toolkit (GTDB-Tk) (v1.0.2), which uses a set 120 universal bacterial gene markers<sup>60</sup>.

576

577 For each taxonomic group, we selected at least two representative sequence types (for a total of  
578 138 genomes), from which we inferred a Maximum likelihood phylogenetic tree based on the core  
579 gene alignment using RAxML (v8.2.11)<sup>61</sup>. The core genome was estimated using panX (v1.5.1).

580 Core genes were defined as those genes present in at least the 80% of sampled genomes (e-value  
581 < 0.005)<sup>62</sup>. Each of the resulting 62 core genes was alignment using muscle (v3.8.3)<sup>63</sup>. Filter.seqs  
582 from mothur (v1.41.3) was used to remove the gaps per each gene alignment<sup>64</sup>. Individual  
583 alignments were concatenated into a single alignment (16,400 bp long) input into RAxML.

584

585 **Assessment of the *Microcystis* genotype diversity in freshwater colonies**

586 A core genome was also estimated for the 109 *Microcystis* genomes and 122 NCBI references  
587 genomes (Supplementary Table 1 and 12). The resulting alignment of the 115 core genes was  
588 degaped (68,145 bp long) and used to infer an ML phylogeny using RAxML. Two outgroups  
589 (*Anabaena variabilis* ATCC29413 and *Synechocystis* sp. PCC6803) were included. Based on ANI  
590 values greater or equal to 99%, the monophyletic clades of *Microcystis* genomes were classified  
591 into 18 genotypes (Supplementary Table 2).

592

593 **Assessment of the *Microcystis* genomic (within-colonies) variation versus intra-genotype  
594 variation (between colonies)**

595 We first confirmed that *Microcystis* is haploid, as polyploidy has been observed among other  
596 cyanobacteria<sup>65</sup>. We estimated ploidy variation in *Microcystis* colonies using k-mer frequencies  
597 and raw sequences. We first mapped the reads of each colony (containing reads from both  
598 *Microcystis* and its microbiome) to a *Microcystis* reference genome using BBmap with minimum  
599 nucleotide identity of 99%<sup>66</sup>. Mapped reads were extracted using Picard  
600 (<http://broadinstitute.github.io/picard/>) and analyzed using Genomescope and Smudgeplot  
601 (<https://github.com/tbenavil/genomescope2.0>; <https://github.com/KamilSJaron/smudgeplot>). All  
602 colonies appeared to be haploid, with a low rate of heterozygosity that could be due paralogs.

603

604 To determine whether *Microcystis* colonies likely formed by clonal cell division or cell  
605 aggregation, we called single nucleotide variants (SNVs) within colonies and between colonies of  
606 the same genotype. As a point of comparison, we also called SNVs that occurred over a period of  
607 approximately six years in laboratory cultures of *Microcystis* with genome sequences reported  
608 previously<sup>29</sup>. We used snippy (v4.4.0) (<https://github.com/tseemann/snippy>) with default  
609 parameters to call SNVs. Genotypes represented by only one sampled colony were excluded from  
610 the analysis (G02, G04, G09, G11, G12, G16, and G18).

611

612 SNV calling within and between colonies was executed by mapping reads against reference  
613 genomes. This was done independently for each genotype. We selected at least four reference  
614 genomes per genotype when possible. SNVs within colonies were detected by mapping the reads  
615 of the references to their respective genome assemblies. SNVs between colonies were detected by  
616 mapping the reads of different colonies of the same genotype to the genome assemblies of the  
617 references. We ignored positions where the reference nucleotide was poorly supported (threshold  
618 percentage for the minor variant <14.4%; mean = 1.1%) by the reads in both the within- and  
619 between-colony read mapping analyses because these were considered to be assembly errors.

620

## 621 **Identifying associated bacterial genomes in colonies**

622 Non-*Microcystis* MAGs from each colony were classified in 72 species based on taxonomical  
623 analysis and ANI values  $\geq 96\%$ . Because individual assemblies could affect MAG completeness,  
624 we created a custom database of the 59 associated bacterial genomes from Quebec, and another  
625 database for the 18 species from Brazil. Using MIDAS (v1.3.0)<sup>67</sup>, we mapped the reads from each

626 colony (downsampled to 8,000,000 reads per colony) against the custom databases to estimate the  
627 relative abundance and coverage for each of the 72 associated bacterial species. We defined a  
628 species to be present when it had a genome-wide average coverage of 1X or more. This allowed  
629 us to generate a matrix of associated bacteria presence or absence across colonies.

630

631 ***Microcystis*' microbiome composition variation according to environmental variables and**  
632 **host genotype**

633 We first performed a distance-based RDA with the square root of the Bray-Curtis distance from a  
634 coverage table describing the composition of the *Microcystis* microbiome for each genotype. The  
635 variables included genotype information, presence/absence of *mcy* genes, temperature, pH, site  
636 (Canada or Brazil) and the temporal variables years and months. In a second approach, we  
637 calculated the beta diversity using the same dissimilarity distance and tested *Microcystis*  
638 microbiome composition variation using adonis() and betadisper().

639

640 We quantified phylosymbiosis by comparing the phylogenetic distance matrix of *Microcystis*  
641 genotypes and the microbiome composition distance matrix using a Mantel test (999 permutations,  
642 Spearman correlation) and the protest() R function to test the non-randomness between these two  
643 matrices (999 permutations) (vegan R package). The pairwise phylogenetic distances matrix was  
644 estimated using the RAxML tree of the *Microcystis* core genome and the cophenetic.phylo  
645 function of the ape R-package (v5.3)<sup>68</sup>.

646

647 ***Microcystis* genotypic diversity from metagenomic samples**

648 *Microcystis* genomes from Quebec and Brazil were classified into 14 and four genotypes,  
649 respectively. This genotype classification was based on pairwise genome similarities greater or  
650 equal to 99%. Using the *Microcystis* genotypes and the software MIDAS (v1.3.0)<sup>67</sup>, we built two  
651 custom gene marker databases for the *Microcystis* genotypes (15 universal single-copy gene  
652 families), one for genotypes from Quebec and the other for genotypes from Brazil.

653

654 Using MIDAS and the custom databases, we estimated the relative abundances, the read counts  
655 and the read coverage of the *Microcystis* genotypes in 72 shotgun metagenomes from Lake  
656 Champlain, Quebec (62 metagenomes from a long-term experiment (2006 to 2016, excluding 2007  
657 and 2014), plus 10 metagenomes from 2017 and 2018). Due the low number of *Microcystis*  
658 genotypes and metagenomes (6 sampling points for Brazil during 2018) from Brazil, these samples  
659 were not formally analyzed. Metagenomic reads with similarity greater or equal to 99% were  
660 mapped against the MIDAS database of *Microcystis* genotypes. We used 14,000,000 reads per  
661 metagenome after downsampling to the lowest-coverage metagenome (Supplementary Table 3).  
662 The metagenome sequencing from Brazil were mapped against a separate MIDAS database of the  
663 four *Microcystis* genotypes from Brazil (Supplementary Fig. 12).

664

665 To test if the 14 *Microcystis* genotypes represented in the colony genomes representative of the  
666 diversity present in the Lake Champlain metagenomes, we first mapped the downsampled  
667 metagenomic reads to a custom database including a single reference *Microcystis* genome  
668 (M083S1) (alignment identity cutoff = 96%), and also mapped the reads to the database including  
669 all the 14 genotypes (alignment identity cutoff = 99%). By using a cutoff value equal to 96%, we  
670 expect to recover most sequences from the *Microcystis* genus, regardless of which genotype the

671 reads come from. We recovered 102,608 reads at 99% identity and 109,729 at 96%, showing that  
672 the 14 genotypes (defined at 99% identity) account for 93.5% of the *Microcystis* reads in the  
673 metagenome samples. Additionally, we observed that the total coverage using all the *Microcystis*  
674 genotypes (alignment identity cutoff = 99%) and the total coverage using a single *Microcystis*  
675 genome as a reference (alignment identity cutoff = 96%) are nearly perfectly correlated  
676 (correlation coefficient  $R^2 = 1$ ,  $P < 2.2\text{e-}16$ ) (Spearman correlation) (Supplementary Fig. 13).

677

#### 678 ***Microcystis* genotypic diversity variation according to environmental variables**

679 To determine the variables that explain the variation in *Microcystis* community composition, we  
680 used a dataset of 42 metagenomes and 14 genotypes from Lake Champlain. Metagenomes with  
681 incomplete metadata were excluded. We focused on Lake Champlain as we observed a greater  
682 diversity of *Microcystis* genotypes compared to Brazil, including both microcystin-producing and  
683 non-producing genotypes. We first used a distance-based redundancy analysis (dbRDA) with the  
684 square root of the Bray Curtis distance matrix to investigate *Microcystis*–environment  
685 relationships<sup>69,70</sup> (capscale function from vegan R package, (v2.5.6l)<sup>71</sup>). Variables were pre-  
686 selected using the ordiR2step R function<sup>72</sup> (See Supplementary Methods). The environmental  
687 matrix variables included: total phosphorus in  $\mu\text{g/l}$  (TP), total nitrogen in  $\mu\text{g/l}$  (TN), soluble  
688 reactive phosphorus in  $\mu\text{g/l}$  (DP), dissolved nitrogen in  $\mu\text{g/l}$  (DN), 1-week-cumulative  
689 precipitation in mm, 1-week-average air temperature in Celsius, temporal variables (Years,  
690 Months and Season) and sampling sites within Lake Champlain (Pelagic or Littoral)  
691 (Supplementary Table 3)<sup>43</sup>. To determine the significance of constraints, we used the anova.cca()  
692 function from the R vegan package.

693 We also calculated the beta diversity between groups of samples using the Phyloseq R package  
694 (v1.30.0) and the square root of Bray Curtis distance. We used nonmetric multi- dimensional  
695 scaling (NMDS, from the phyloseq package that incorporates the metaMDS() function from the R  
696 vegan<sup>71,73,74</sup> package to ordinate the data. Differences in community structure between groups were  
697 tested using permutational multivariate analysis of variance (PERMANOVA<sup>75</sup>) with the adonis()  
698 function. As PERMANOVA tests might be sensitive to dispersion, we also tested for dispersion  
699 by performing an analysis of multivariate homogeneity (PERMDISP<sup>76</sup>) with the permuted  
700 betadisper() function.

701

702 **Identifying the correlation between microbiome members and *Microcystis* in freshwater  
703 samples from Canada**

704 Using the 59 species identified in the *Microcystis* microbiome from Canada and the software  
705 MIDAS (v1.3.0), we built a custom gene marker database of 15 universal single-copy gene  
706 families. This database also included a reference genome from *Microcystis* (M083S1) and two  
707 *Dolichospermum* reference genomes (*D. circinale* AWQC131C and AWQC310F). Using MIDAS,  
708 we estimated the relative abundances, reads count, and the read coverage of each associated  
709 bacterial species in 72 shotgun metagenomes from Quebec, Canada. Reads were mapped against  
710 the custom database including the associated bacteria species. A cuff-off value of nucleotide  
711 identity greater or equal to 96% was used for the read mapping. By merging the values (coverage  
712 and read counts) for species within the same genus, obtained coverage and read counts at the genus  
713 level, for 32 genera of associated bacteria. We used the Spearman rank-based correlation to  
714 investigate patterns of co-occurrence between *Microcystis*, *Dolichospermum* and the associated  
715 bacterial species and genera in environmental metagenomes. First, the read counts in the matrices

716 containing the genera and species were used to estimate the correlation values ( $r$ ) and p-values  
717 between pair of species or genera by using the rcorr() function of the Hmisc (v4.3.0) R package<sup>77</sup>.  
718 We also calculated Spearman correlations on the coverage values, yielding similar results.  $P$ -  
719 values were corrected to control the false discovery rate using the qvalue() function from the  
720 qvalue (v2.18.0) R package. We also estimated the correlation between *Microcystis* and the AB  
721 using the software FastSpar (v0.0.10)<sup>78</sup>. This method is a faster implementation of the Sparse  
722 Correlation for Compositional Data algorithm (SparCC)<sup>79</sup>. The significance of the test was  
723 evaluated using 100 permutations and a bootstrap of 1000. In general, the most prevalent AB taxa  
724 in *Microcystis* colonies had significant correlation ( $P < 0.05$ ) with *Microcystis* using both  
725 Spearman and SparCC.

726

## 727 **Co-phylogeny between *Microcystis* and the associated microbiome**

728 The nine most prevalent associated bacterial genera were selected for co-phylogeny analysis,  
729 which would be underpowered to detect phylogenetic associations with low-prevalence bacteria  
730 (i.e. small phylogenies). Core genomes were generated using panX and core alignments were  
731 computed as described above, for each associated bacterial genus. Phylogenetic core genome trees  
732 were built individually for each genus using RAxML<sup>61</sup>. Patristic distances (pairwise distances  
733 between pairs of tips on a tree) for the *Microcystis* and associated bacteria phylogenies were  
734 estimated using the cophenetic.phylo() function from the ape R-package<sup>68</sup>. The *Microcystis* core  
735 genome tree and the tree of the associated bacteria were compared using Parafit test (parafit()  
736 function of the ape R package) (See Supplementary Methods)<sup>68,80</sup>. Co-phylogeny trees were built  
737 using the function cophylo() from the phytools R package<sup>81</sup>.

738

739 **Recent HGT between *Microcystis* and associated bacteria (AB)**

740 To infer recent horizontal gene transfer (HGT) events between *Microcystis* and associated bacteria,  
741 we first inferred the pangenomes for each combination of one AB and *Microcystis*, and repeated  
742 this for the 72 associated bacterial species. Core and accessory genes with a minimum percentage  
743 identity for blastp equal to 99% were identified. We retained those clusters of genes present in at  
744 least four genomes, and present in both AB and *Microcystis*. The remaining putatively horizontal  
745 transferred genes were annotated in 23 COG (clusters of orthologous groups) categories using  
746 eggNOG-mapper (v2.0.1)<sup>82</sup>. Using the package STAMP (v2.1.3) and a chi-square test, we  
747 estimated if there were statistical differences in the COG categories between *Microcystis* core  
748 genes and the putative horizontally transferred genes<sup>83</sup>. P-values were corrected using Benjamini-  
749 Hochberg (controlling the false discovery rate) method. We also estimated HGT events between  
750 *Microcystis* and associated species using a second method, Metachip (v1.8.2) (default parameters).  
751 The Metachip approach uses both the best match approach (blastn) and a phylogenetic approach  
752 to infer HGT (reconciliation between a gene tree and its species tree)<sup>37</sup>.

753

754 **Gene functional annotation**

755 The *Microcystis* and associated bacteria genomes were functionally annotated using enrichM  
756 (v0.5.0) (<https://github.com/geronimp/enrichM>)<sup>84</sup>. A PCA based on the presence/absence of  
757 KEGG Orthologous genes (KO) in *Microcystis* and associated bacteria genera was generated using  
758 the option 'enrichment' in enrichM. Genome groups (*Microcystis* vs each associated bacteria  
759 genus) were compared using the same option. KEGG modules differentially abundant in  
760 *Microcystis* or the associated bacteria genus were filtered based on a completeness greater or equal  
761 to 70%.

762

763 *Microcystis* and associated bacterial genomes (109 *Microcystis* and 391 associated genomes) were  
764 annotated using Roary (v3.13.0). The resulting genomes in GenBank format were used to predict  
765 the biosynthetic gene clusters (BGCs) using default parameters (--taxon bacteria --cb-general --  
766 cb-knownclusters --cb-subclusters --ASF --pfam2go --smcog-trees --genefinding-tool prodigal-m)  
767 in antiSMASH (v5.1.2)<sup>85,86</sup>. The BiG-SCAPE package (v1.0.1) with default parameters analysed  
768 the ANTISMASH BGCs and based on a similarity network classified them into Gene Cluster  
769 Families (GCFs)<sup>87</sup>. BGCs were classified in BiG-SCAPE classes (e.g., polyketide synthases  
770 nonribosomal peptide synthetases (NRPSs), post-translationally modified peptides (RiPPs) and  
771 terpenes. A total of 2,395 BGCs were identified in 415 genomes.

772

### 773 **Data availability**

774

775 Raw sequences and metagenome assembled genomes (MAGs) are available in NCBI under  
776 Bioproject numbers PRJNA507251 and PRJNA662092.

777

### 778 **References**

779

- 780 1 Levesque, B. *et al.* Prospective study of acute health effects in relation to exposure to  
781 cyanobacteria. *Sci Total Environ* **466-467**, 397-403, doi:10.1016/j.scitotenv.2013.07.045  
782 (2014).
- 783 2 Bell, W. & Mitchell, R. Chemotactic and growth responses of marine bacteria to algal  
784 extracellular products. *Biological Bulletin* **143**, 265-277, doi:10.2307/1540052 (1972).

785 3 Seymour, J. R., Amin, S. A., Raina, J. B. & Stocker, R. Zooming in on the phycosphere:  
786 the ecological interface for phytoplankton-bacteria relationships. *Nat Microbiol* **2**, 17065,  
787 doi:10.1038/nmicrobiol.2017.65 (2017).

788 4 Amin, S. A., Parker, M. S. & Armbrust, E. V. Interactions between diatoms and bacteria.  
789 *Microbiol Mol Biol Rev* **76**, 667-684, doi:10.1128/MMBR.00007-12 (2012).

790 5 Paerl, H. W. Microscale physiological and ecological studies of aquatic cyanobacteria:  
791 macroscale implications. *Microsc Res Tech* **33**, 47-72, doi:10.1002/(SICI)1097-  
792 0029(199601)33:1<47::AID-JEMT6>3.0.CO;2-Y (1996).

793 6 Cho, D. H. *et al.* Enhancing microalgal biomass productivity by engineering a microalgal-  
794 bacterial community. *Bioresour Technol* **175**, 578-585,  
795 doi:10.1016/j.biortech.2014.10.159 (2015).

796 7 Amin, S. A. *et al.* Interaction and signalling between a cosmopolitan phytoplankton and  
797 associated bacteria. *Nature* **522**, 98-101, doi:10.1038/nature14488 (2015).

798 8 Van Mooy, B. A. *et al.* Quorum sensing control of phosphorus acquisition in  
799 *Trichodesmium* consortia. *ISME J* **6**, 422-429, doi:10.1038/ismej.2011.115 (2012).

800 9 Frischkorn, K. R., Rouco, M., Van Mooy, B. A. S. & Dyhrman, S. T. Epibionts dominate  
801 metabolic functional potential of *Trichodesmium* colonies from the oligotrophic ocean.  
802 *ISME J* **11**, 2090-2101, doi:10.1038/ismej.2017.74 (2017).

803 10 Paerl, H. W. Growth and reproductive strategies of freshwater blue-green algae  
804 (Cyanobacteria). *Growth and reproductive strategies of freshwater phytoplankton*, 261-  
805 315 (1988).

806 11 Worm, J. & Sondergaard, M. Dynamics of heterotrophic bacteria attached to *Microcystis*  
807 spp. (Cyanobacteria). *Aquat Microb Ecol* **14**, 19-28, doi:10.3354/ame014019 (1998).

808 12 Brunberg, A. K. Contribution of bacteria in the mucilage of *Microcystis* spp.  
809 (Cyanobacteria) to benthic and pelagic bacterial production in a hypereutrophic lake. *Fems*  
810 *Microbiol Ecol* **29**, 13-22, doi:10.1016/S0168-6496(98)00126-3 (1999).

811 13 Parveen, B. *et al.* Bacterial communities associated with *Microcystis* colonies differ from  
812 free-living communities living in the same ecosystem. *Environ Microbiol Rep* **5**, 716-724,  
813 doi:10.1111/1758-2229.12071 (2013).

814 14 Jankowiak, J. G. & Gobler, C. J. The composition and function of microbiomes within  
815 *Microcystis* colonies are significantly different than native bacterial assemblages in two  
816 North American lakes. *Front Microbiol* **11**, doi:10.3389/fmicb.2020.01016 (2020).

817 15 Dziallas, C. & Grossart, H. P. Temperature and biotic factors influence bacterial  
818 communities associated with the cyanobacterium *Microcystis* sp. *Environ Microbiol* **13**,  
819 1632-1641, doi:10.1111/j.1462-2920.2011.02479.x (2011).

820 16 Cook, K. V. *et al.* The global *Microcystis* interactome. *Limnol Oceanogr* **65**, S194-S207,  
821 doi:10.1002/lno.11361 (2020).

822 17 Shia, L. M. *et al.* Community structure of bacteria associated with *Microcystis* colonies  
823 from cyanobacterial blooms. *J Freshwater Ecol* **25**, 193-203,  
824 doi:10.1080/02705060.2010.9665068 (2010).

825 18 Berg, K. A. *et al.* High diversity of cultivable heterotrophic bacteria in association with  
826 cyanobacterial water blooms. *ISME J* **3**, 314-325, doi:10.1038/ismej.2008.110 (2009).

827 19 Shen, H., Niu, Y., Xie, P., Tao, M. & Yang, X. Morphological and physiological changes  
828 in *Microcystis aeruginosa* as a result of interactions with heterotrophic bacteria.  
829 *Freshwater Biol* **56**, 1065-1080, doi:10.1111/j.1365-2427.2010.02551.x (2011).

830 20 Wang, W. J. *et al.* Experimental evidence for the role of heterotrophic bacteria in the  
831 formation of *Microcystis* colonies. *J Appl Phycol* **28**, 1111-1123, doi:10.1007/s10811-015-  
832 0659-5 (2016).

833 21 Xiao, M., Willis, A., Burford, M. A. & Li, M. Review: a meta-analysis comparing cell-  
834 division and cell-adhesion in *Microcystis* colony formation. *Harmful Algae* **67**, 85-91,  
835 doi:10.1016/j.hal.2017.06.007 (2017).

836 22 Lim, S. J. & Bordenstein, S. R. An introduction to phylosymbiosis. *Proc Biol Sci* **287**,  
837 20192900, doi:10.1098/rspb.2019.2900 (2020).

838 23 Groussin, M. *et al.* Unraveling the processes shaping mammalian gut microbiomes over  
839 evolutionary time. *Nat Commun* **8**, 14319, doi:10.1038/ncomms14319 (2017).

840 24 Yeoh, Y. K. *et al.* Evolutionary conservation of a core root microbiome across plant phyla  
841 along a tropical soil chronosequence. *Nat Commun* **8**, 215, doi:10.1038/s41467-017-  
842 00262-8 (2017).

843 25 Pollock, F. J. *et al.* Coral-associated bacteria demonstrate phylosymbiosis and  
844 cophylogeny. *Nat Commun* **9**, 4921, doi:10.1038/s41467-018-07275-x (2018).

845 26 Mazel, F. *et al.* Is host filtering the main driver of phylosymbiosis across the tree of life?  
846 *mSystems* **3**, doi:10.1128/mSystems.00097-18 (2018).

847 27 Groussin, M., Mazel, F. & Alm, E. J. Co-evolution and co-speciation of host-gut bacteria  
848 systems. *Cell Host Microbe* **28**, 12-22, doi:10.1016/j.chom.2020.06.013 (2020).

849 28 Harke, M. J. *et al.* A review of the global ecology, genomics, and biogeography of the toxic  
850 cyanobacterium, *Microcystis* spp. *Harmful Algae* **54**, 4-20, doi:10.1016/j.hal.2015.12.007  
851 (2016).

852 29 Perez-Carrascal, O. M. *et al.* Coherence of *Microcystis* species revealed through population  
853 genomics. *ISME J* **13**, 2887-2900, doi:10.1038/s41396-019-0481-1 (2019).

854 30 Jackrel, S. L. *et al.* Genome evolution and host-microbiome shifts correspond with  
855 intraspecific niche divergence within harmful algal bloom-forming *Microcystis*  
856 *aeruginosa*. *Mol Ecol* **28**, 3994-4011, doi:10.1111/mec.15198 (2019).

857 31 Wilson, A. E. *et al.* Genetic variation of the bloom-forming cyanobacterium *Microcystis*  
858 *aeruginosa* within and among lakes: implications for harmful algal blooms. *Appl Environ*  
859 *Microbiol* **71**, 6126-6133, doi:10.1128/AEM.71.10.6126-6133.2005 (2005).

860 32 Dittmann, E., Neilan, B. A., Erhard, M., vonDohren, H. & Borner, T. Insertional  
861 mutagenesis of a peptide synthetase gene that is responsible for hepatotoxin production in  
862 the cyanobacterium *Microcystis aeruginosa* PCC 7806. *Mol Microbiol* **26**, 779-787,  
863 doi:10.1046/j.1365-2958.1997.6131982.x (1997).

864 33 Peres-Neto, P. R. & Jackson, D. A. How well do multivariate data sets match? The  
865 advantages of a Procrustean superimposition approach over the Mantel test. *Oecologia* **129**,  
866 169-178, doi:10.1007/s004420100720 (2001).

867 34 Kurmayer, R., Dittmann, E., Fastner, J. & Chorus, I. Diversity of microcystin genes within  
868 a population of the toxic cyanobacterium *Microcystis* spp. in Lake Wannsee (Berlin,  
869 Germany). *Microb Ecol* **43**, 107-118, doi:10.1007/s00248-001-0039-3 (2002).

870 35 Briand, E. *et al.* Spatiotemporal changes in the genetic diversity of a bloom-forming  
871 *Microcystis aeruginosa* (cyanobacteria) population. *ISME J* **3**, 419-429,  
872 doi:10.1038/ismej.2008.121 (2009).

873 36 Smillie, C. S. *et al.* Ecology drives a global network of gene exchange connecting the  
874 human microbiome. *Nature* **480**, 241-244, doi:10.1038/nature10571 (2011).

875 37 Song, W., Wemheuer, B., Zhang, S., Steensen, K. & Thomas, T. MetaCHIP: community-  
876 level horizontal gene transfer identification through the combination of best-match and  
877 phylogenetic approaches. *Microbiome* **7**, 36, doi:10.1186/s40168-019-0649-y (2019).

878 38 Paerl, H. W., Tucker, J. & Bland, P. T. Carotenoid enhancement and its role in maintaining  
879 blue-green algal (*Microcystis aeruginosa*) surface blooms1. *Limnol Oceanogr* **28**, 847-857,  
880 doi:10.4319/lo.1983.28.5.0847 (1983).

881 39 Gerloff, G. C., Fitzgerald, G. P. & Skoog, F. The mineral nutrition of *Microcystis*  
882 *aeruginosa*. *Am J Bot* **39**, 26-32, doi:10.2307/2438090 (1952).

883 40 Tromas, N. *et al.* Niche separation increases with genetic distance among bloom-forming  
884 cyanobacteria. *Front Microbiol* **9**, 438, doi:10.3389/fmicb.2018.00438 (2018).

885 41 Chun, S. J. *et al.* Characterization of distinct cyanoHABs-related modules in microbial  
886 recurrent association network. *Front Microbiol* **10**, doi:10.3389/fmicb.2019.01637 (2019).

887 42 Zhang, Z. *et al.* Alteration of dominant cyanobacteria in different bloom periods caused by  
888 abiotic factors and species interactions. *J Environ Sci* **99**, 1-9,  
889 doi:10.1016/j.jes.2020.06.001 (2021).

890 43 Tromas, N. *et al.* Characterising and predicting cyanobacterial blooms in an 8-year  
891 amplicon sequencing time course. *ISME J* **11**, 1746-1763, doi:10.1038/ismej.2017.58  
892 (2017).

893 44 Xiao, M., Li, M. & Reynolds, C. S. Colony formation in the cyanobacterium *Microcystis*.  
894 *Biol Rev* **93**, 1399-1420, doi:10.1111/brv.12401 (2018).

895 45 Li, Q. *et al.* A large-scale comparative metagenomic study reveals the functional  
896 interactions in six bloom-forming *Microcystis*-epibiont communities. *Front Microbiol* **9**,  
897 746, doi:10.3389/fmicb.2018.00746 (2018).

898 46 Douglas, A. E. & Werren, J. H. Holes in the Hologenome: Why Host-Microbe Symbioses  
899 Are Not Holobionts. *mBio* **7**, e02099, doi:10.1128/mBio.02099-15 (2016).

900 47 Kosourov, S., Murukesan, G., Jokela, J. & Allahverdiyeva, Y. Carotenoid biosynthesis in  
901 *Calothrix* sp. 336/3: Composition of carotenoids on full medium, during diazotrophic  
902 growth and after long-term H<sub>2</sub> photoproduction. *Plant Cell Physiol* **57**, 2269-2282,  
903 doi:10.1093/pcp/pcw143 (2016).

904 48 Pattanaik, B. & Lindberg, P. Terpenoids and their biosynthesis in cyanobacteria. *Life* **5**,  
905 doi:10.3390/life5010269 (2015).

906 49 Beiko, R. G., Harlow, T. J. & Ragan, M. A. Highways of gene sharing in prokaryotes. *Proc  
907 Natl Acad Sci USA* **102**, 14332-14337, doi:10.1073/pnas.0504068102 (2005).

908 50 Morris, J. J., Lenski, R. E. & Zinser, E. R. The Black Queen Hypothesis: evolution of  
909 dependencies through adaptive gene loss. *mBio* **3**, doi:10.1128/mBio.00036-12 (2012).

910 51 Schmidt, K. C., Jackrel, S. L., Smith, D. J., Dick, G. J. & Denef, V. J. Genotype and host  
911 microbiome alter competitive interactions between *Microcystis aeruginosa* and *Chlorella  
912 sorokiniana*. *Harmful Algae* **99**, 101939, doi:<https://doi.org/10.1016/j.hal.2020.101939>  
913 (2020).

914 52 Bolger, A. M., Lohse, M. & Usadel, B. Trimmomatic: a flexible trimmer for Illumina  
915 sequence data. *Bioinformatics* **30**, 2114-2120, doi:10.1093/bioinformatics/btu170 (2014).

916 53 Li, D. *et al.* MEGAHIT v1.0: A fast and scalable metagenome assembler driven by  
917 advanced methodologies and community practices. *Methods* **102**, 3-11,  
918 doi:10.1016/j.ymeth.2016.02.020 (2016).

919 54 Eren, A. M. *et al.* Anvi'o: an advanced analysis and visualization platform for 'omics data.  
920 *PeerJ* **3**, e1319, doi:10.7717/peerj.1319 (2015).

921 55 Parks, D. H., Imelfort, M., Skennerton, C. T., Hugenholtz, P. & Tyson, G. W. CheckM:  
922 assessing the quality of microbial genomes recovered from isolates, single cells, and  
923 metagenomes. *Genome Res* **25**, 1043-1055, doi:10.1101/gr.186072.114 (2015).

924 56 Bowers, R. M. *et al.* Minimum information about a single amplified genome (MISAG) and  
925 a metagenome-assembled genome (MIMAG) of bacteria and archaea. *Nat Biotechnol* **35**,  
926 725-731, doi:10.1038/nbt.3893 (2017).

927 57 Seemann, T. Prokka: rapid prokaryotic genome annotation. *Bioinformatics* **30**, 2068-2069,  
928 doi:10.1093/bioinformatics/btu153 (2014).

929 58 Jain, C., Rodriguez, R. L., Phillippy, A. M., Konstantinidis, K. T. & Aluru, S. High  
930 throughput ANI analysis of 90K prokaryotic genomes reveals clear species boundaries. *Nat*  
931 *Commun* **9**, 5114, doi:10.1038/s41467-018-07641-9 (2018).

932 59 Pritchard, L., Glover, R. H., Humphris, S., Elphinstone, J. G. & Toth, I. K. Genomics and  
933 taxonomy in diagnostics for food security: soft-rotting enterobacterial plant pathogens.  
934 *Analytical Methods* **8**, 12-24, doi:10.1039/C5AY02550H (2016).

935 60 Chaumeil, P. A., Mussig, A. J., Hugenholtz, P. & Parks, D. H. GTDB-Tk: a toolkit to  
936 classify genomes with the Genome Taxonomy Database. *Bioinformatics*,  
937 doi:10.1093/bioinformatics/btz848 (2019).

938 61 Stamatakis, A. *et al.* RAxML-Light: a tool for computing terabyte phylogenies.  
939 *Bioinformatics* **28**, 2064-2066, doi:10.1093/bioinformatics/bts309 (2012).

940 62 Ding, W., Baumdicker, F. & Neher, R. A. panX: pan-genome analysis and exploration.  
941 *Nucleic Acids Res* **46**, e5, doi:10.1093/nar/gkx977 (2018).

942 63 Edgar, R. C. MUSCLE: a multiple sequence alignment method with reduced time and  
943 space complexity. *BMC Bioinformatics* **5**, 113, doi:10.1186/1471-2105-5-113 (2004).

944 64 Schloss, P. D. *et al.* Introducing mothur: open-source, platform-independent, community-  
945 supported software for describing and comparing microbial communities. *Appl Environ  
946 Microbiol* **75**, 7537-7541, doi:10.1128/AEM.01541-09 (2009).

947 65 Griese, M., Lange, C. & Soppa, J. Ploidy in cyanobacteria. *Fems Microbiol Lett* **323**, 124-  
948 131, doi:10.1111/j.1574-6968.2011.02368.x (2011).

949 66 Bushnell, B. *BBMap: A Fast, Accurate, Splice-Aware Aligner*. (Lawrence Berkeley  
950 National Lab (LBNL), Berkeley, CA, 2014).

951 67 Nayfach, S., Rodriguez-Mueller, B., Garud, N. & Pollard, K. S. An integrated  
952 metagenomics pipeline for strain profiling reveals novel patterns of bacterial transmission  
953 and biogeography. *Genome Res* **26**, 1612-1625, doi:10.1101/gr.201863.115 (2016).

954 68 Paradis, E., Claude, J. & Strimmer, K. APE: Analyses of phylogenetics and evolution in R  
955 language. *Bioinformatics* **20**, 289-290, doi:10.1093/bioinformatics/btg412 (2004).

956 69 Bray, J. R. & Curtis, J. T. An ordination of the upland forest communities of southern  
957 Wisconsin. *Ecol Monogr* **27**, 325-349, doi:10.2307/1942268 (1957).

958 70 Legendre, P. & Anderson, M. J. Distance-based redundancy analysis: testing multispecies  
959 responses in multifactorial ecological experiments. *Ecol Monogr* **69**, 1-24,  
960 doi:10.1890/0012-9615(1999)069[0001:DBRATM]2.0.CO;2 (1999).

961 71 Oksanen, J. *et al.* Vegan: Community Ecology Package. (2019).

962 72 Blanchet, F. G., Legendre, P. & Borcard, D. Forward selection of explanatory variables.  
963 *Ecology* **89**, 2623-2632, doi:Doi 10.1890/07-0986.1 (2008).

964 73 Shepard, R. N. The Analysis of Proximities - Multidimensional-Scaling with an Unknown  
965 Distance Function .1. *Psychometrika* **27**, 125-140, doi:Doi 10.1007/Bf02289630 (1962).

966 74 Kruskal, J. B. Multidimensional-Scaling by Optimizing Goodness of Fit to a Nonmetric  
967 Hypothesis. *Psychometrika* **29**, 1-27, doi:Doi 10.1007/Bf02289565 (1964).

968 75 Anderson, M. J. A new method for non-parametric multivariate analysis of variance.  
969 *Austral Ecol* **26**, 32-46, doi:DOI 10.1046/j.1442-9993.2001.01070.x (2001).

970 76 Anderson, M. J. Distance-based tests for homogeneity of multivariate dispersions.  
971 *Biometrics* **62**, 245-253, doi:10.1111/j.1541-0420.2005.00440.x (2006).

972 77 Harrell, J. F. & Dupont, C. *Hmisc: harrell miscellaneous. R package version 4.1-1*.  
973 <https://CRAN.R-project.org/package=Hmisc>.

974 78 Watts, S. C., Ritchie, S. C., Inouye, M. & Holt, K. E. FastSpar: rapid and scalable  
975 correlation estimation for compositional data. *Bioinformatics* **35**, 1064-1066,  
976 doi:10.1093/bioinformatics/bty734 (2019).

977 79 Friedman, J. & Alm, E. J. Inferring correlation networks from genomic survey data. *PLoS  
978 Comput Biol* **8**, e1002687, doi:10.1371/journal.pcbi.1002687 (2012).

979 80 Legendre, P., Desdevises, Y. & Bazin, E. A statistical test for host-parasite coevolution.  
980 *Syst Biol* **51**, 217-234, doi:10.1080/10635150252899734 (2002).

981 81 Revell, L. J. Phytools: an R package for phylogenetic comparative biology (and other  
982 things). *Methods Ecol Evol* **3**, 217-223, doi:10.1111/j.2041-210X.2011.00169.x (2012).

983 82 Huerta-Cepas, J. *et al.* eggNOG 5.0: a hierarchical, functionally and phylogenetically  
984 annotated orthology resource based on 5090 organisms and 2502 viruses. *Nucleic Acids  
985 Res* **47**, D309-D314, doi:10.1093/nar/gky1085 (2019).

986 83 Parks, D. H., Tyson, G. W., Hugenholtz, P. & Beiko, R. G. STAMP: statistical analysis of  
987 taxonomic and functional profiles. *Bioinformatics* **30**, 3123-3124,  
988 doi:10.1093/bioinformatics/btu494 (2014).

989 84 Boyd, J. A. *et al.* Divergent methyl-coenzyme M reductase genes in a deep-subseafloor  
990 Archaeoglobi. *ISME J* **13**, 1269-1279, doi:10.1038/s41396-018-0343-2 (2019).  
991 85 Blin, K. *et al.* antiSMASH 4.0-improvements in chemistry prediction and gene cluster  
992 boundary identification. *Nucleic Acids Res* **45**, W36-W41, doi:10.1093/nar/gkx319 (2017).  
993 86 Blin, K. *et al.* antiSMASH 5.0: updates to the secondary metabolite genome mining  
994 pipeline. *Nucleic Acids Res* **47**, W81-W87, doi:10.1093/nar/gkz310 (2019).  
995 87 Navarro-Munoz, J. C. *et al.* A computational framework to explore large-scale biosynthetic  
996 diversity. *Nat Chem Biol* **16**, 60-68, doi:10.1038/s41589-019-0400-9 (2020).  
997

## 998 **Acknowledgements**

999  
1000 We are grateful to Julie Marleau, Miria Elias and Alberto Mazza for assistance in the sampling.  
1001 This work was supported by the Genome Québec and Genome Canada-funded ATRAPP Project  
1002 (Algal blooms, Treatment, Risk Assessment, Prediction and Prevention). Colonies and water  
1003 samples from Brazil were obtained thanks to a FAPEMIG grant to A.G. We also want to  
1004 acknowledge the financial support of the National Research Council.  
1005

## 1006 **Author contributions**

1007  
1008 B.J.S., N.T. and O.M.P.C. designed the study. O.M.P.C., N.T., A.G., L.C.B.M. and N.F. performed  
1009 the lab experiments. N.T. and O.M.P.C. performed the data analyses. E.M. and O.M.P.C.  
1010 performed the cophylogeny. B.J.S., N.T. and O.M.P.C. wrote the manuscript. B.J.S., N.T.,  
1011 O.M.P.C., A.G., Y.T. and N.F. contributed to its reviewing and editing.

1012

1013 **Competing interests**

1014 The authors declare no conflict of interest.

1015